Almost-Impossible Materials Science by 3D Diffraction Microscopy

Ian McNulty

BESSY / Advanced Photon Source

16 June 2006

Outline

Motivation

Resolution and 3D

Coherent methods

The need for speed

Future directions

The challenge

- The capability to image structure in 3D at the molecular scale and beyond is essential to solve many problems in materials science
- Electron microscopes, STMs, AFMs, etc., are superb tools but are limited to surfaces and thin films
- X-ray crystallography is not, but depends on crystalline samples
- Lenses limit the resolution of conventional x-ray microscopes, and 3D methods are impractically slow for many experiments.

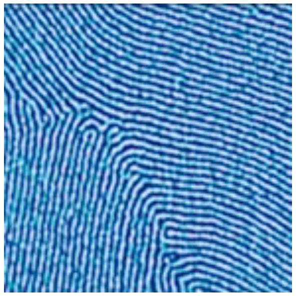

How can we reach beyond these limits?

We need better tools to study ordering

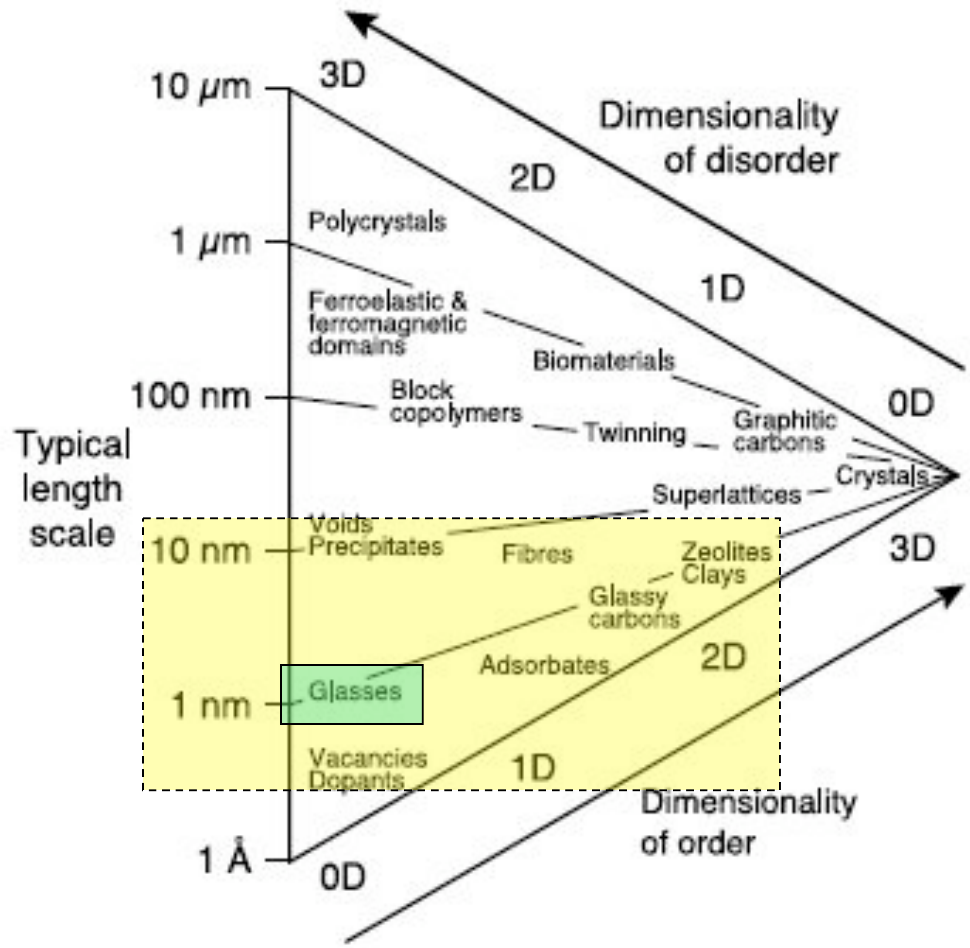

Figure 1. Typical length scales and dimensionality of disorder in some classes of materials. The disorder in most materials is usually defined relative to a lattice. Glasses are an exception, where short range order is determined by nearest neighbour bond distances and interbond angles.

M. Treacy et al., *Rep. Prog. Phys.* 68, 2899 (2005)

Aerogels form interconnected networks

A.. Roshi, S. Barjami, G. Iannacchione (Worchester Polytechnic Inst.)

Aerosils and gels form long, necklace-like, chains that interconnect randomly and percolate with fractal dimensions. Dynamics and fluctuations are modified by phase transitions in surrounding matrix (e.g., smectic-phase liquid crystal)

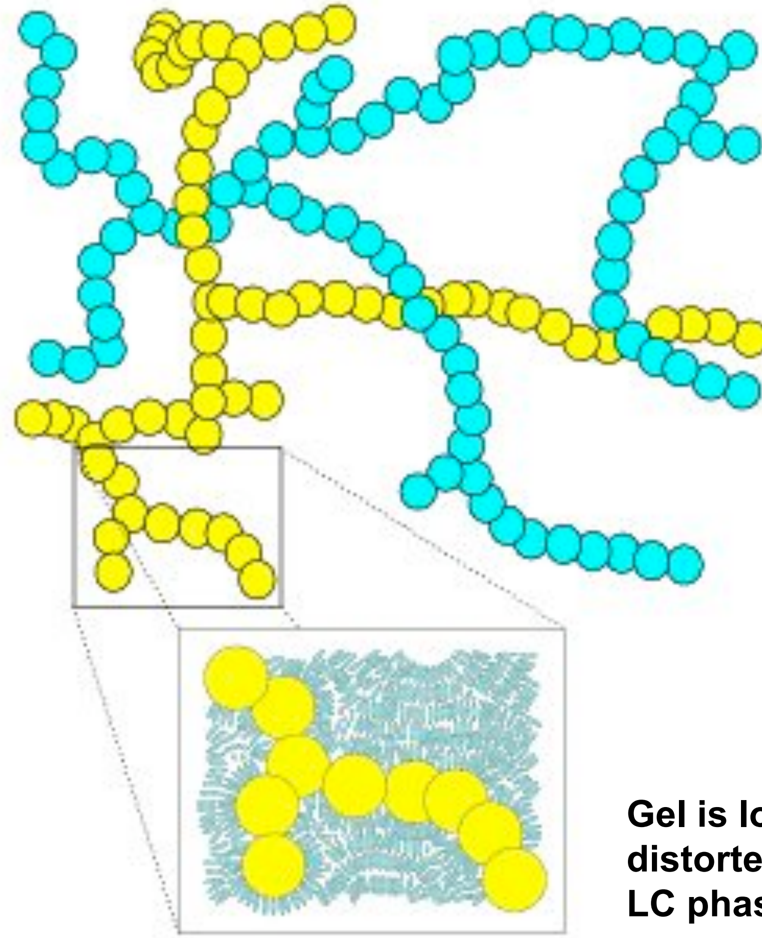

Gel is locally distorted by LC phase

Block Copolymer directed Hybrids in Bulk

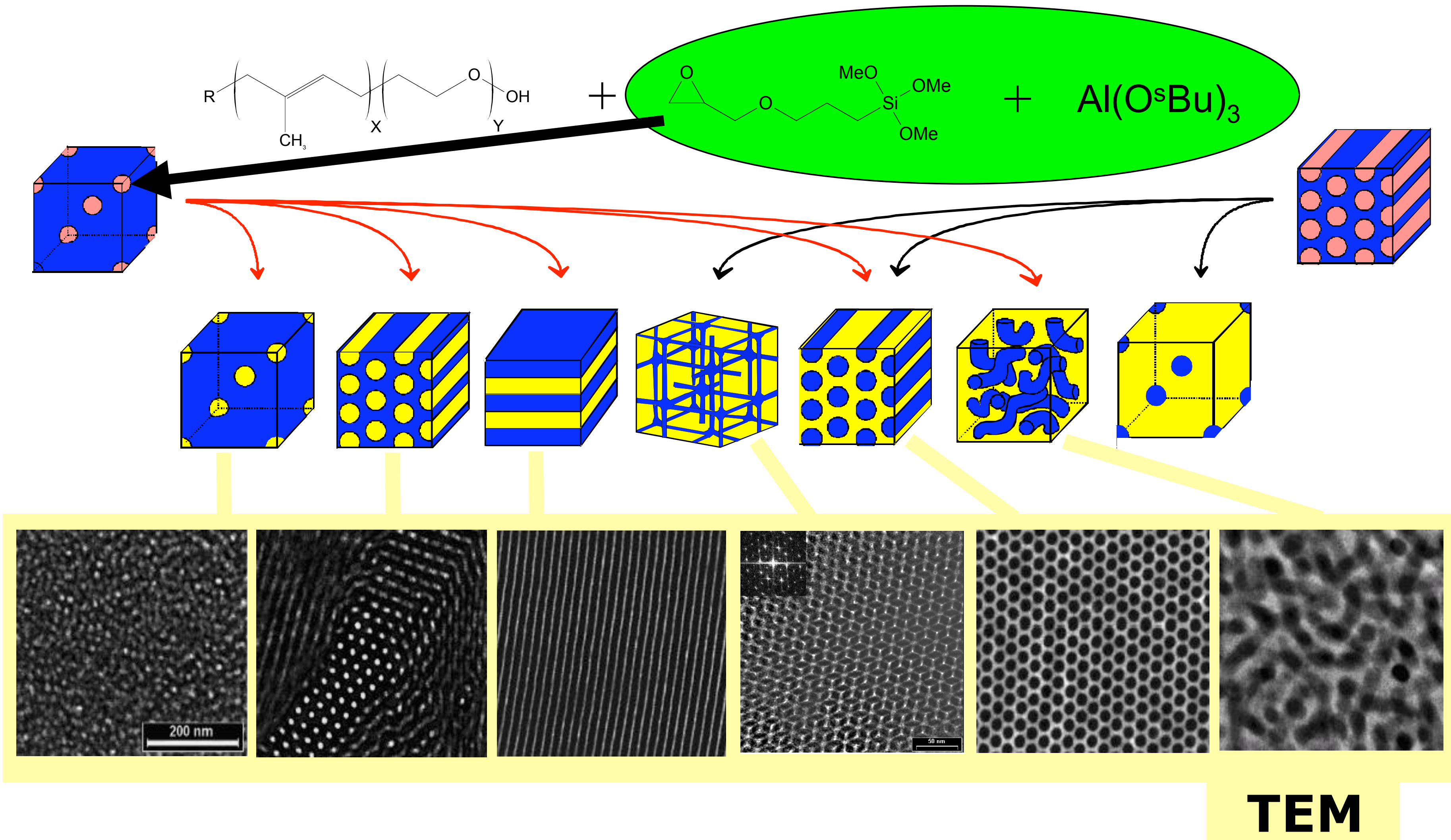

R. Ulrich, A. Du Chesne, M. Templin, U. Wiesner, *Adv. Mater.* 11, 141 (1999)

Cr antiferromagnetic domain evolution

Diffraction contrast shows regions with different magnetic order

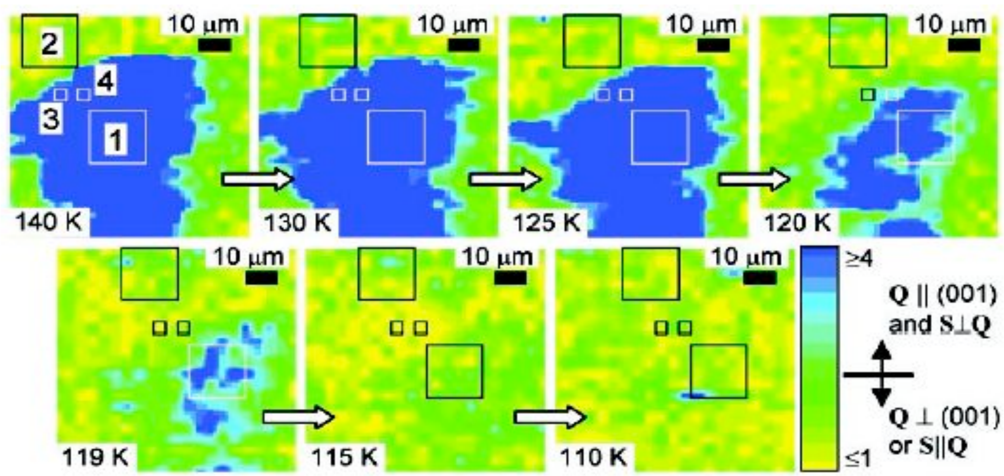

Spin-flip transition T_{SF} is non-uniform within domain

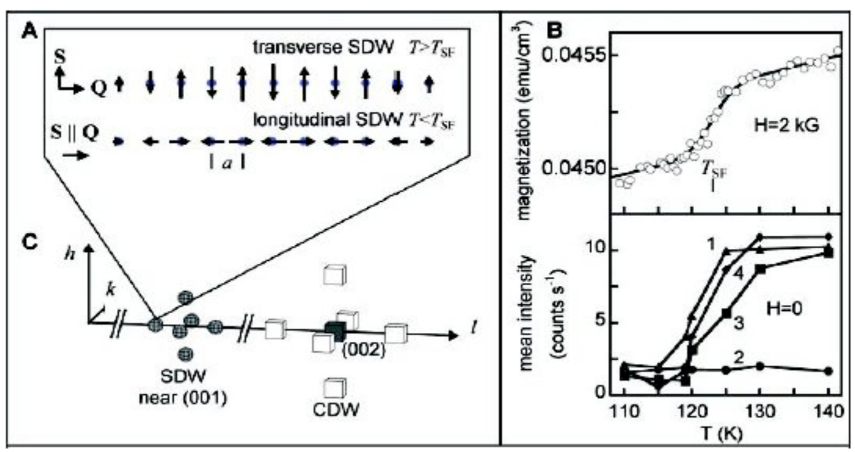

P. Evans et al.,
Science 295, 1042 (2002)

Need brilliance to get intense, small spot

Flux per spatially coherent mode

$F_c = B\, \lambda^2/4$

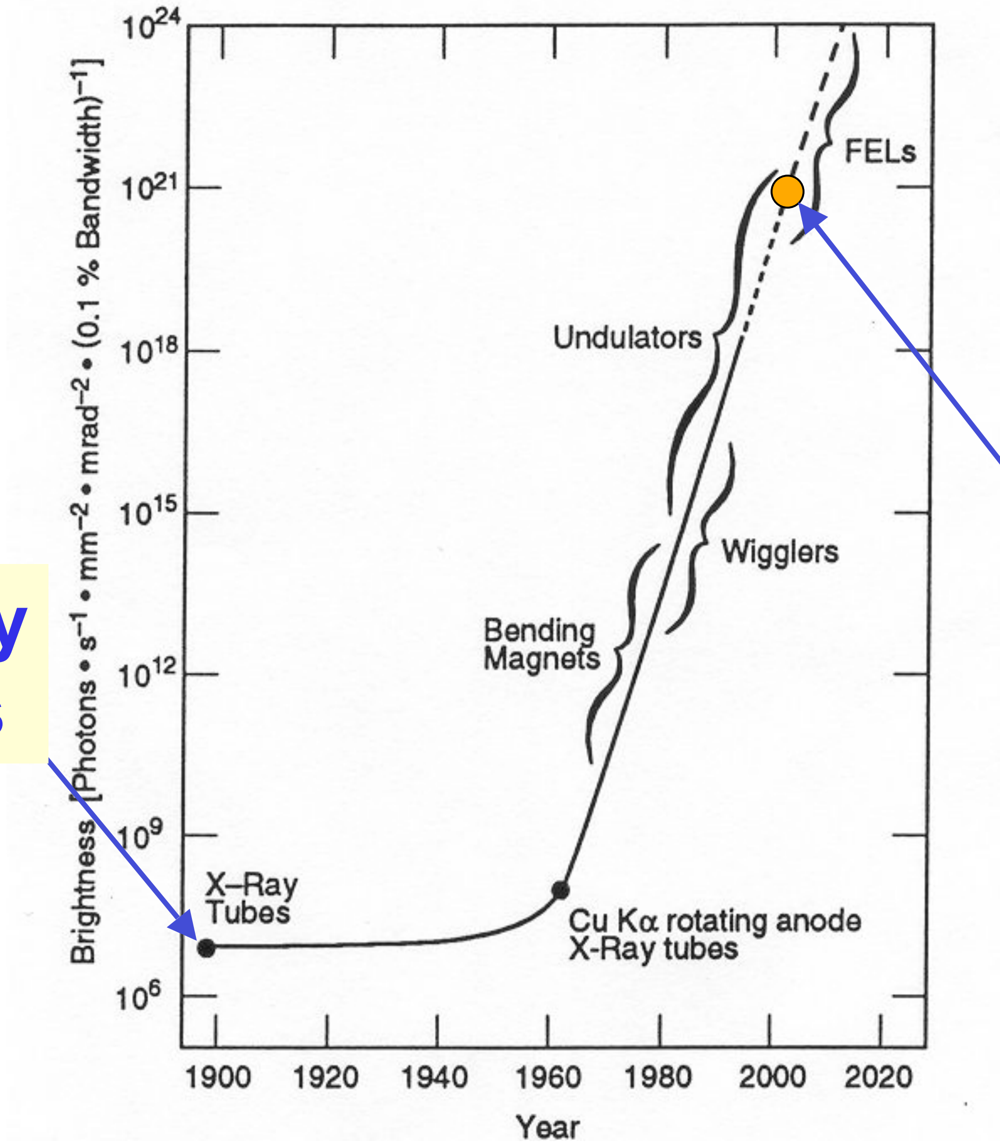

Discovery of x-rays

We are here

H. Winick, "Synchrotron Radiation Sources: A Primer," (1994)

What can we uniquely do at the ERL?

Modes:	(A) Flux	(B) High-Coherence	(C) Short-Pulse	(D) Ultra High-Coherence	(E) Ultra Short-Pulse	Unit
		Short-Term Goals		Long-Term Goals		
Energy	5	5	5	5	5	GeV
Macropulse current	100	25	1	100	1	mA
Bunch charge	77	19	1000	77	10000	pC
Repetition rate	1300	1300	1	1300	0.1	MHz
Transverse emittance (norm. rms)	0.3	0.08	5.0	0.06	5.0	mm.mrad
Transverse emittance (geometric at 5GeV)	31	8.2	511	6.1	511	pm
Bunch length (rms)	2000	2000	50	2000	20	fsec
intrabunch Energy spread (fractional;rms)	2E-4	2E-4	3E-3	2E-4	3E-3	
Beam power	500	125	5	500	5	MW
Beam loss	< 1	< 1	< 1	< 1	< 1	μA

Image formation as a scattering process

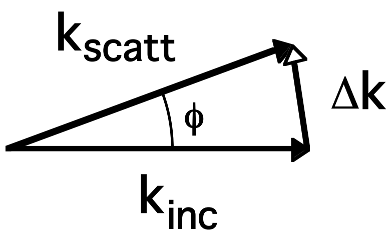

Incident waves with initial momentum k_{inc} are elastically scattered into new direction k_{scatt} with momentum transfer Δk.

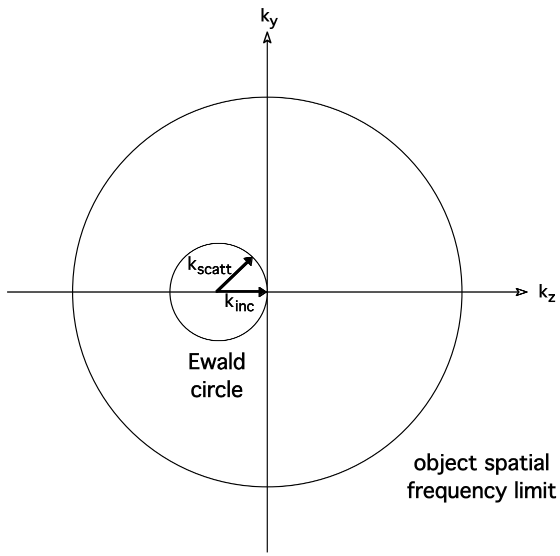

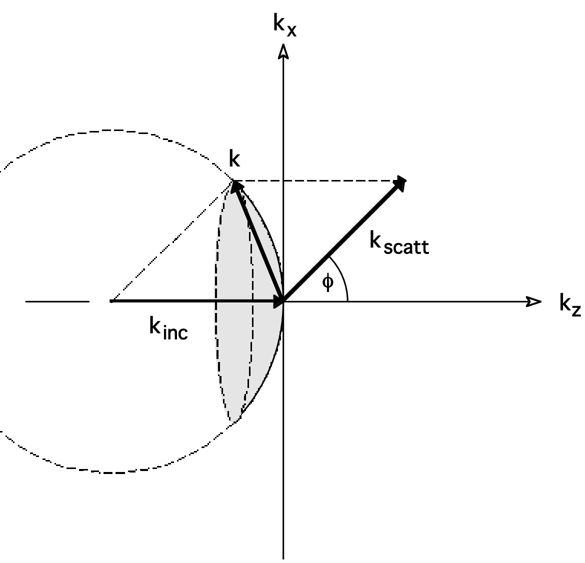

Ewald sphere (2D) defined by conservation of momentum and limit of spatial frequencies in the object defined by object composition. Only spatial frequencies on the Ewald sphere are accessible to the imaging process, limiting attainable resolution.

Diffraction limits to resolution

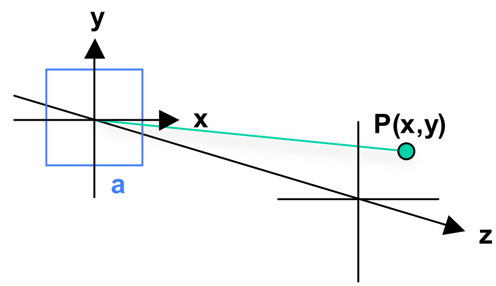

Point-spread function

$$P(x,y) = \frac{\sin x}{x}\,\frac{\sin y}{y}$$

with $x = \dfrac{kax}{z}$, $y = \dfrac{kay}{z}$

Transverse $\boxed{R = 0.5\,\dfrac{\lambda}{NA}}$

where $NA \sim \dfrac{a}{z}$

$$k = \frac{2\pi}{\lambda}$$

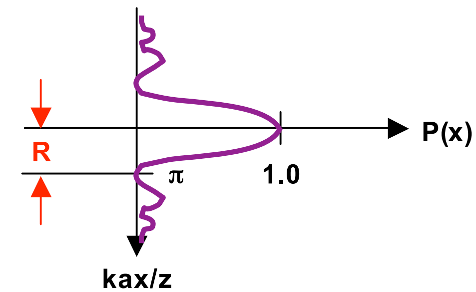

Bragg's law

$\Delta\vec{k} = \vec{k}_{inc} - \vec{k}_{scatt}$ $(0 \le \Delta k \le 2k_{inc})$ $k_x^2 + k_y^2 + (k_z + k_{inc})^2 = k_{inc}^2$

For extreme-angle ray (xz plane, $k_y = 0$) with $k_x = \dfrac{2\pi}{2R} = \dfrac{2\pi}{\lambda}NA$

Longitudinal $\boxed{DOF = \dfrac{\lambda}{(NA)^2}}$ **and** $k_z = \dfrac{k_x^2}{2k_{inc}}$ $(k_z << k_{inc})$

Toward 3D

$R \approx 0.61\ \lambda\ /\ NA$ $DOF \approx 1.22\ \lambda\ /\ (NA)^2\ =\ 2\ R^2\ /\ (0.61\lambda)$

$|n| \approx 1 \quad \Rightarrow \quad NA << 1 \quad \Rightarrow \quad DOF << R$

Synthesize larger NA with multiple views

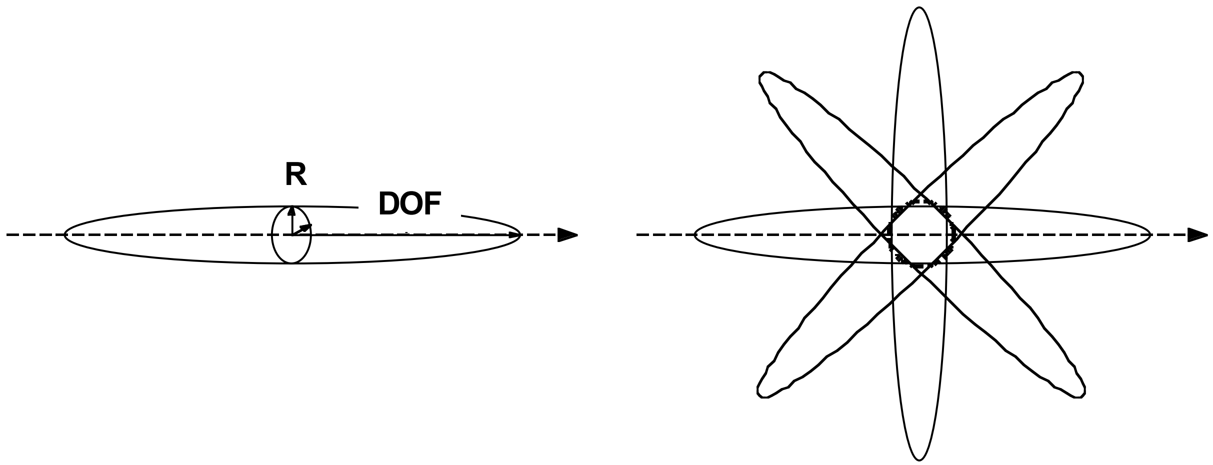

Cannot improve R, only DOF by tomography

Computed tomography

1 **Record many projections through sample over wide angular range. Projections at angles *q* contain:**

$$I(x,y,\theta) = I_0 e^{-\int \mu_\theta (x',y',z')dz'}$$

2 **Reconstruct 3D sample density from suite *S* of projections**

$$\text{Invert } S\{I(x,y,\theta)\} \Rightarrow \mu(x,y,z)$$

X-ray microscopy methods

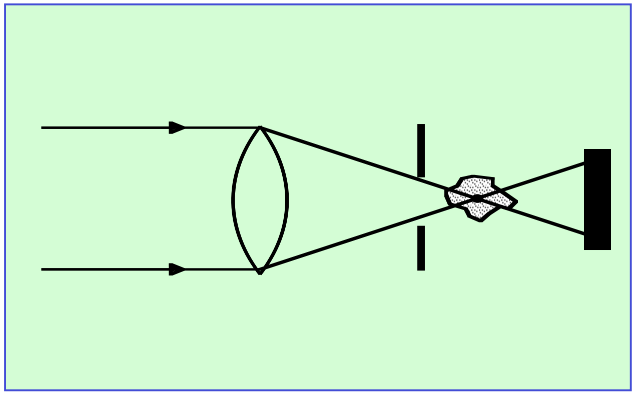

Scanning

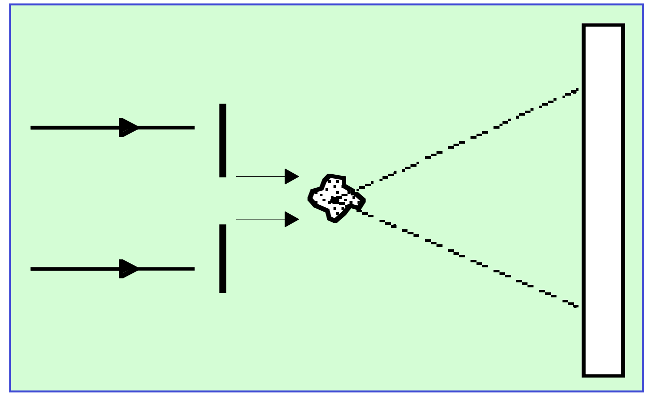

Diffraction

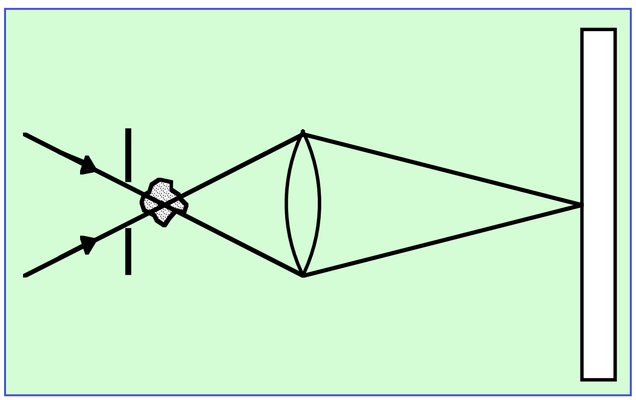

Imaging

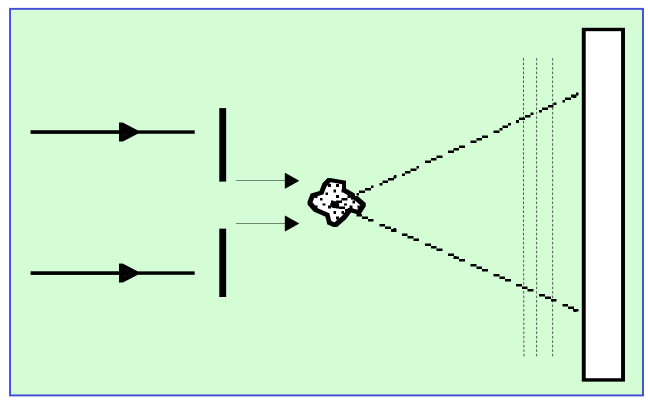

Holography

Scanning x-ray microscopy/tomography

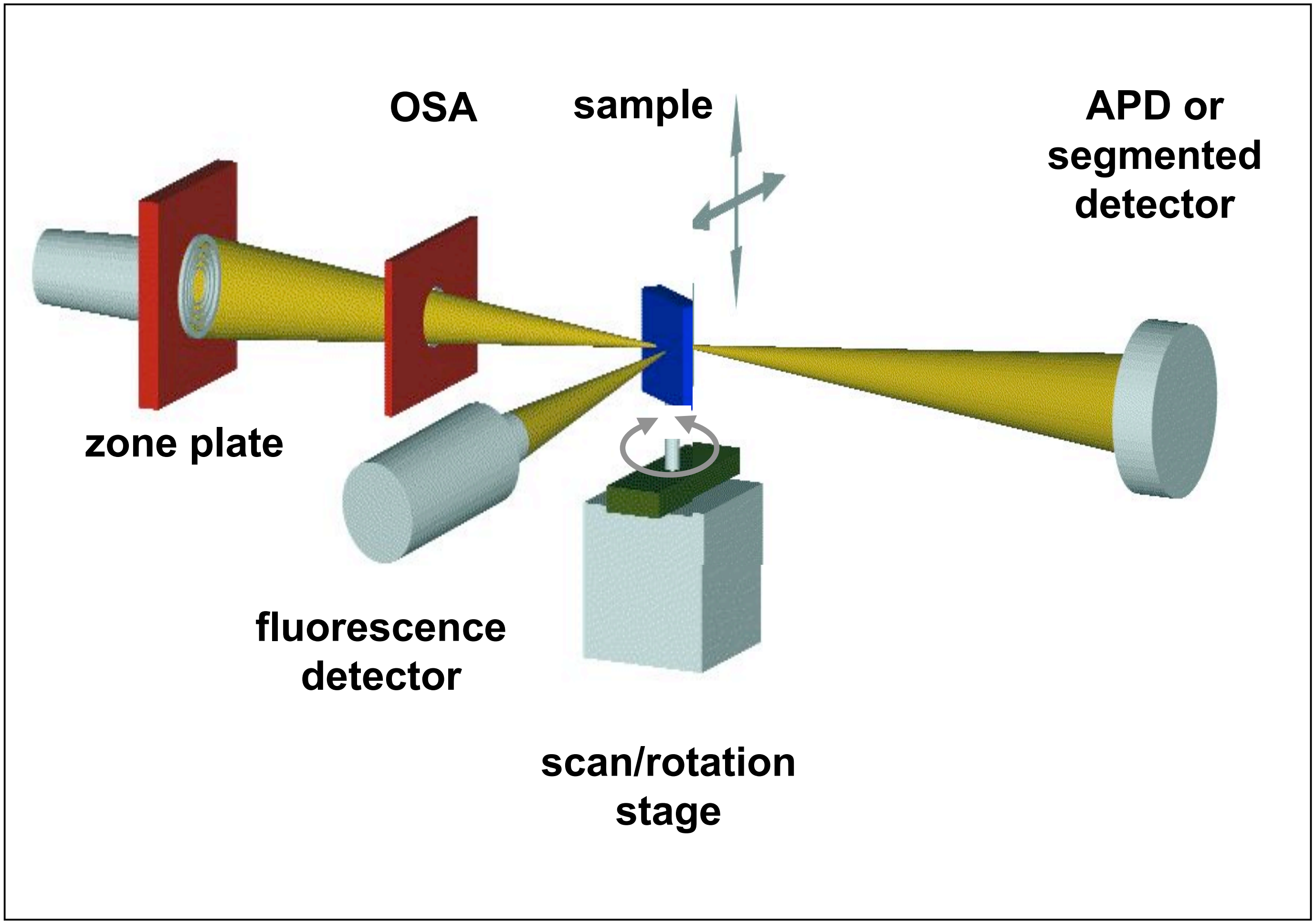

Scanning nanotomography of chips

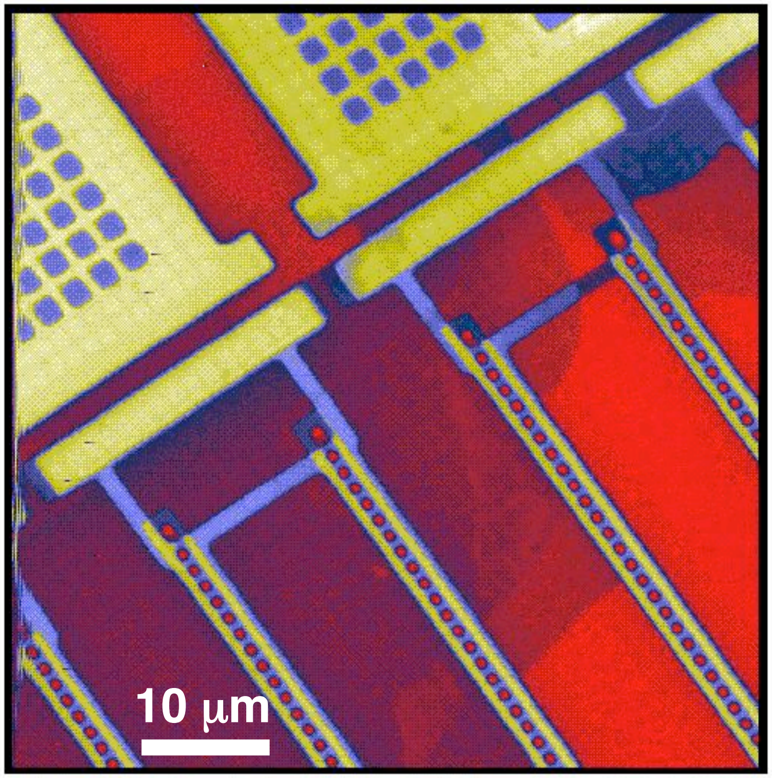

Scanning transmission x-ray micrograph (1830 eV) of a Cu/W/Si test device, showing interconnects and vias.

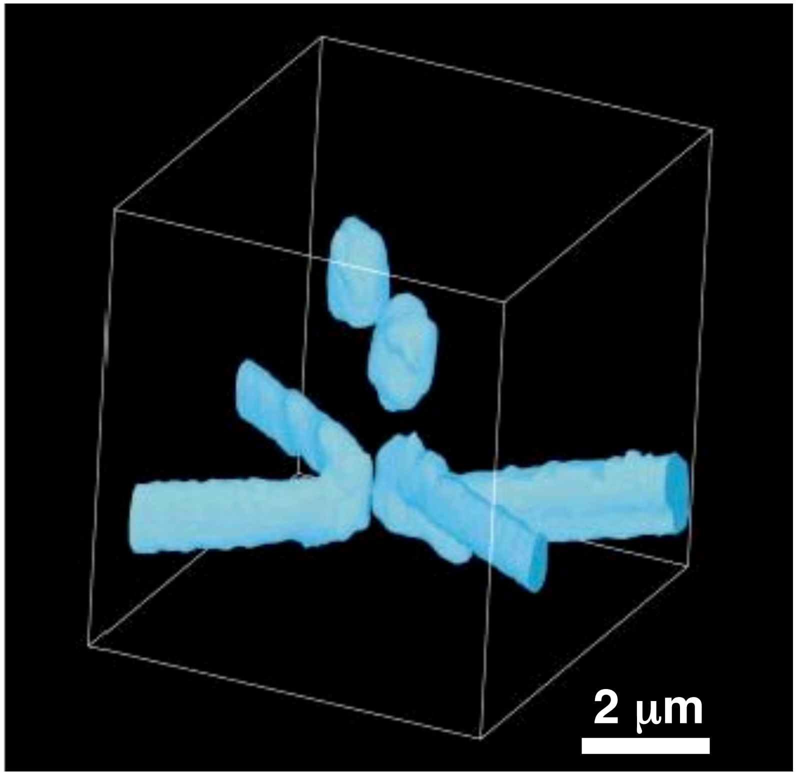

Bayesian reconstruction reconstruction of 13 STXM projections (±69°, 1573 eV) through two-level Al/W/Si test object. Al interconnects are joined by W vias. Two FIB markers are at top.

Z. Levine et al., *Appl. Phys. Lett*. 74, 150 (1999)

Detailed study of electromigration void

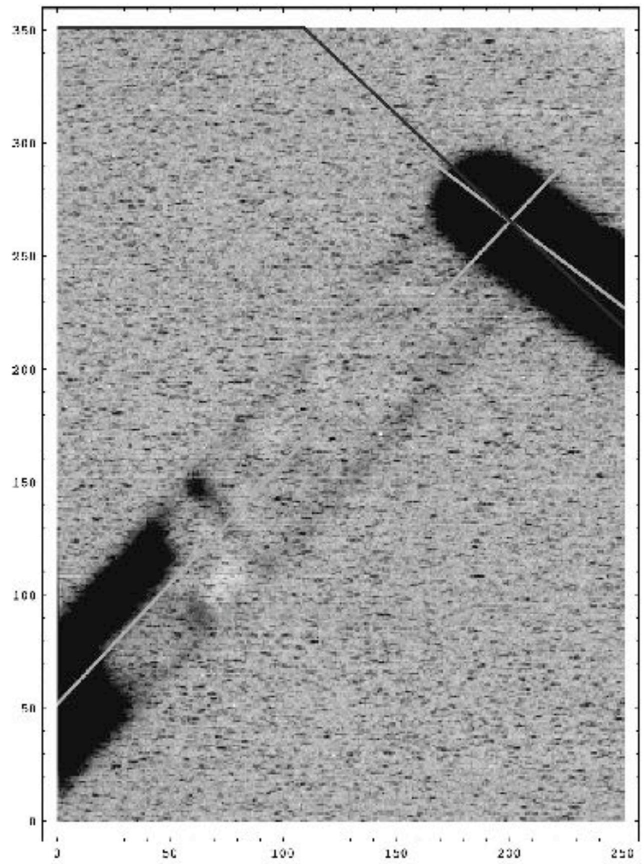

Normal-incidence scan of interconnect showing electromigration void detail.

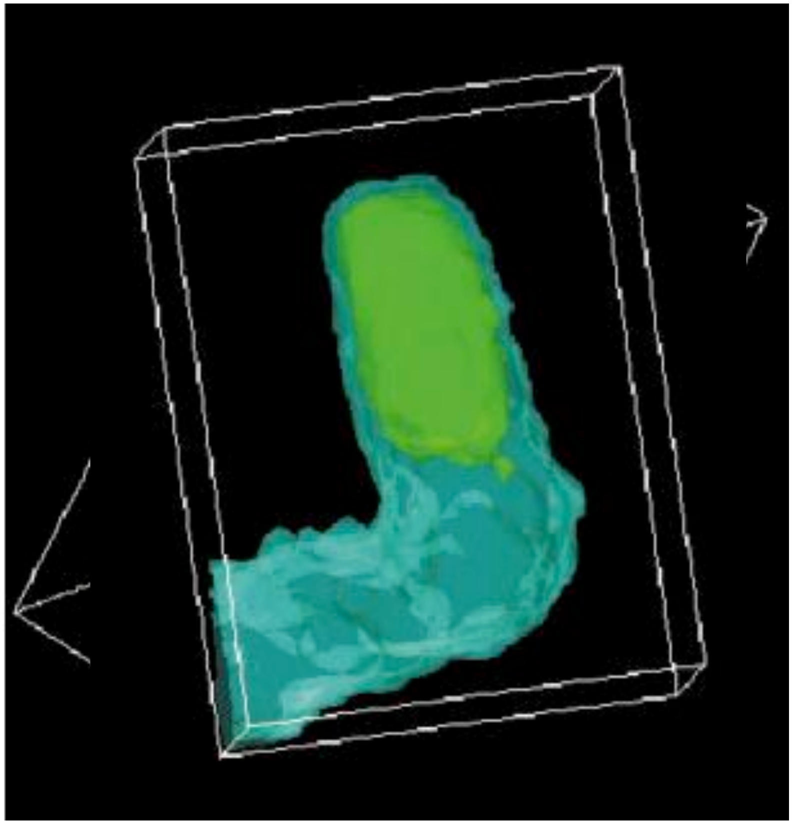

Bayesian reconstruction of ragged end of void

Z. Levine, et al., *J. Appl. Phys.* 87, 4483 (2000)

Quantitative phase tomography

- **Defocus series (a, b, c) and phase (d) of a silicon AFM tip**
- **Quantitative 3D reconstructions of real part of refractive index from ±70° tomographic projections through tip**
- **Calculated $\delta = 5.1 \times 10^{-5}$**

  Measured $\delta = 5.0 \pm 0.5 \times 10^{-5}$

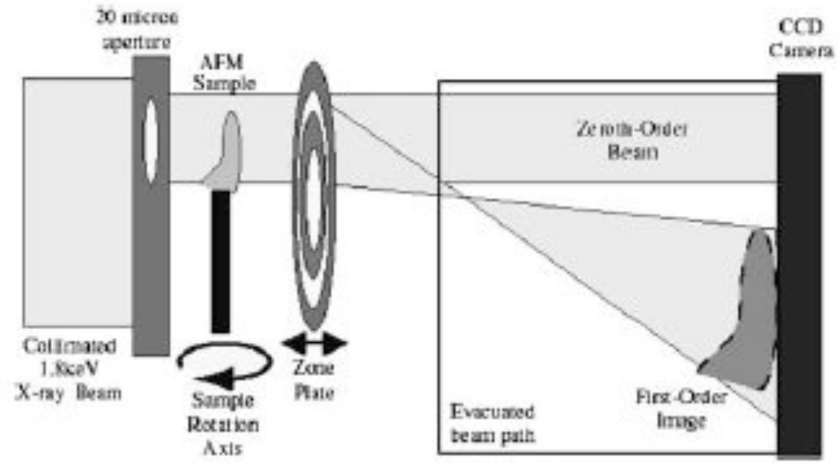

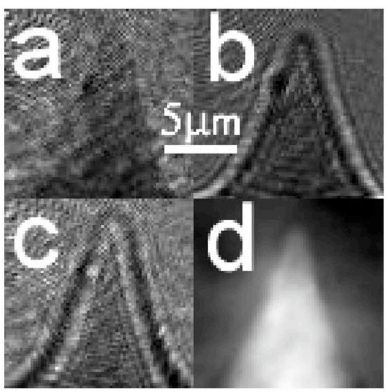

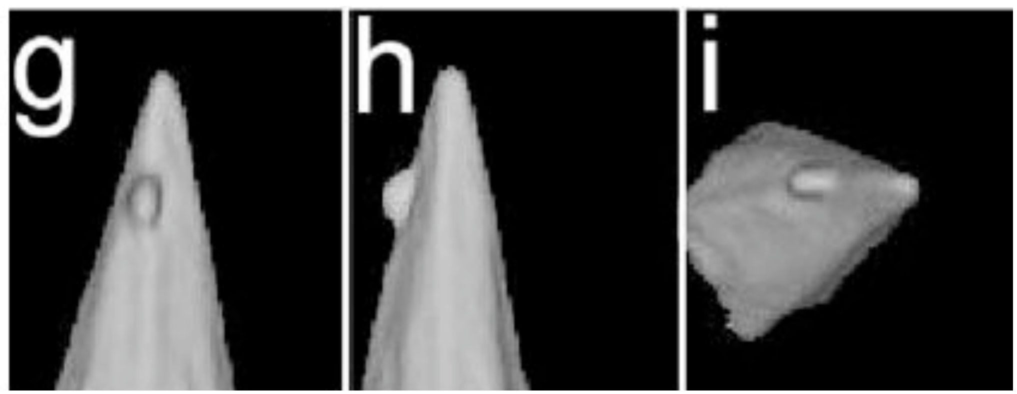

P. McMahon et al., *Opt. Commun.* 217, 53 (2003)

Approaching the limit for focusing x-rays?

1D MLL

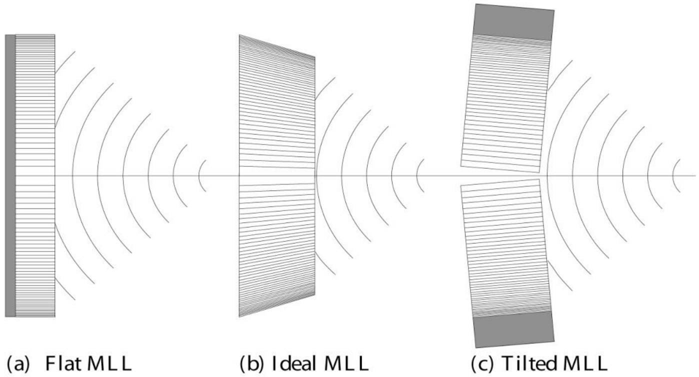

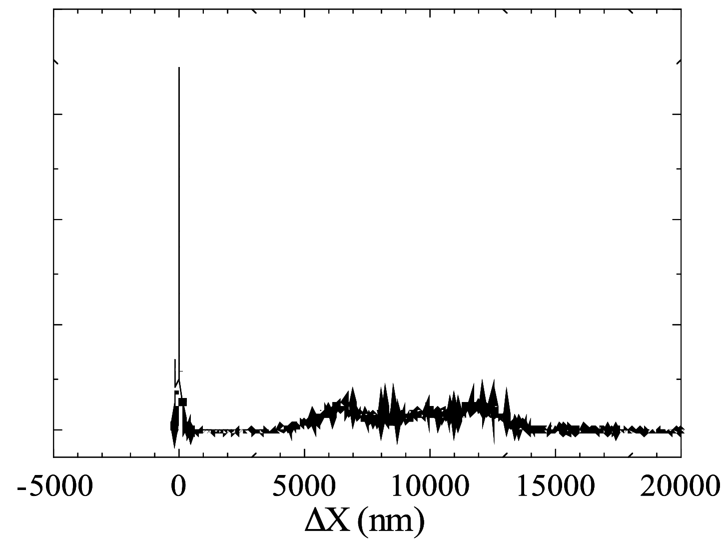

2D MLL

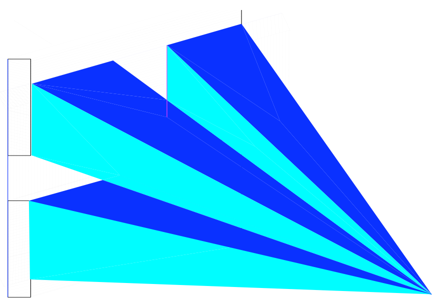

Smallest zone	**dr_N = 10 nm**
NA-limited resolution	**24 nm (41% NA)**
Photon Energy	**19.5 keV**
Measured Resolution (1D)	**30 nm**
Diffraction Efficiency	**44%**

Ideal MLL structure:

- **~1 nm resolution feasible**
- **2D diffraction efficiency > 50%**

Tilted MLL: 5 nm resolution feasible

Kang et al., *Phys. Rev. Lett.* 96, 127401 (2006)

Optics limitations

Achieving high NA is challenging because x-rays interact weakly

$n = 1 - \delta - i\beta$ $\delta,\beta \sim 10^{-3}$ to 10^{-6} $\Rightarrow$ $|n| \approx 1$

Refractive (compound refractive lenses) ~ 50 nm

Low efficiency, highly chromatic, significant aberrations

Reflective (Kirkpatrick-Baez mirrors) ~ 40 nm

High efficiency, achromatic, but limited to ~10 nm by Q_c

Diffractive (Fresnel zone plates, MLLs) ~ 18 nm

Limited to ~10 nm by aspect ratio, except MLL

~5 nm ?

Crystal lenses (impractical)

High angular resolution, but insufficient angular coverage

Differential-aperture x-ray microscopy

3D depth-resolved, white-beam Laue diffraction technique

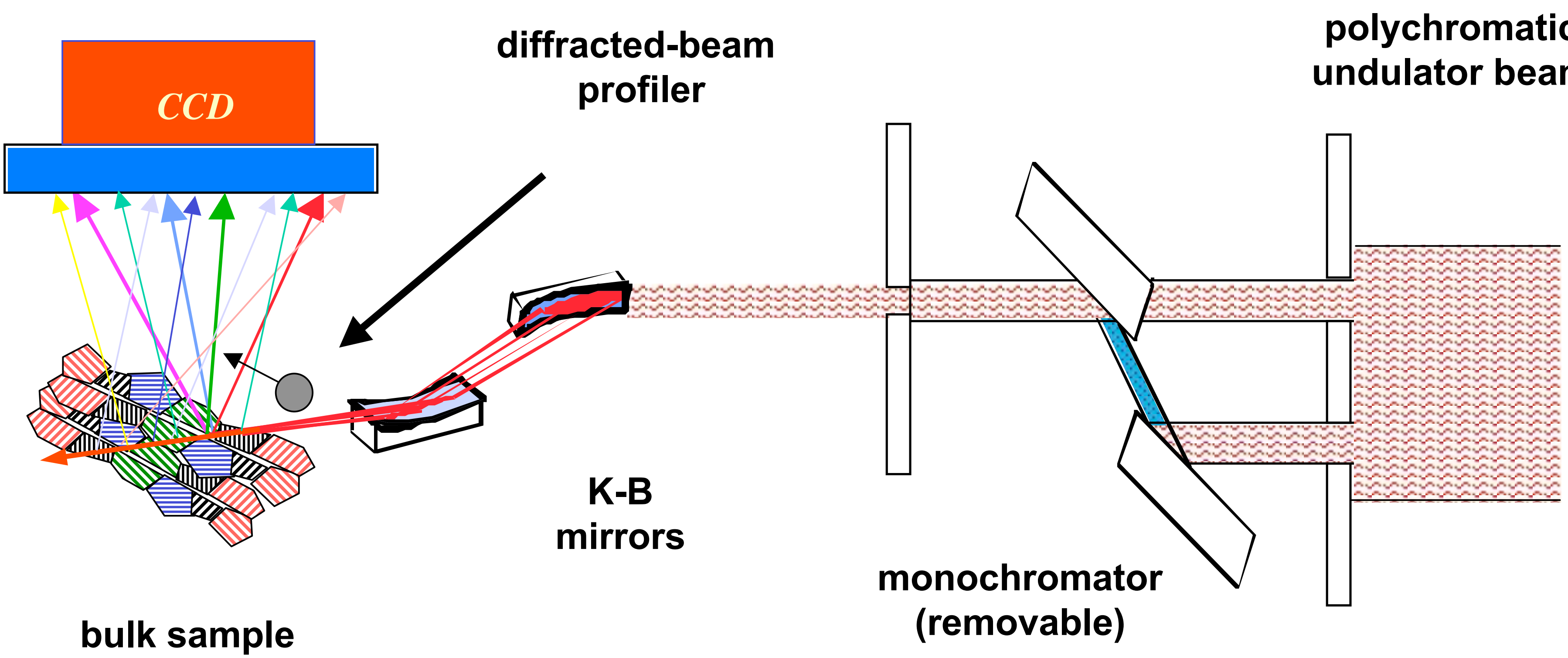

B. Larson, W. Yang, G. Ice, *Nature* 415, 887 (2002)

Studying 3D Al structure by DAXM

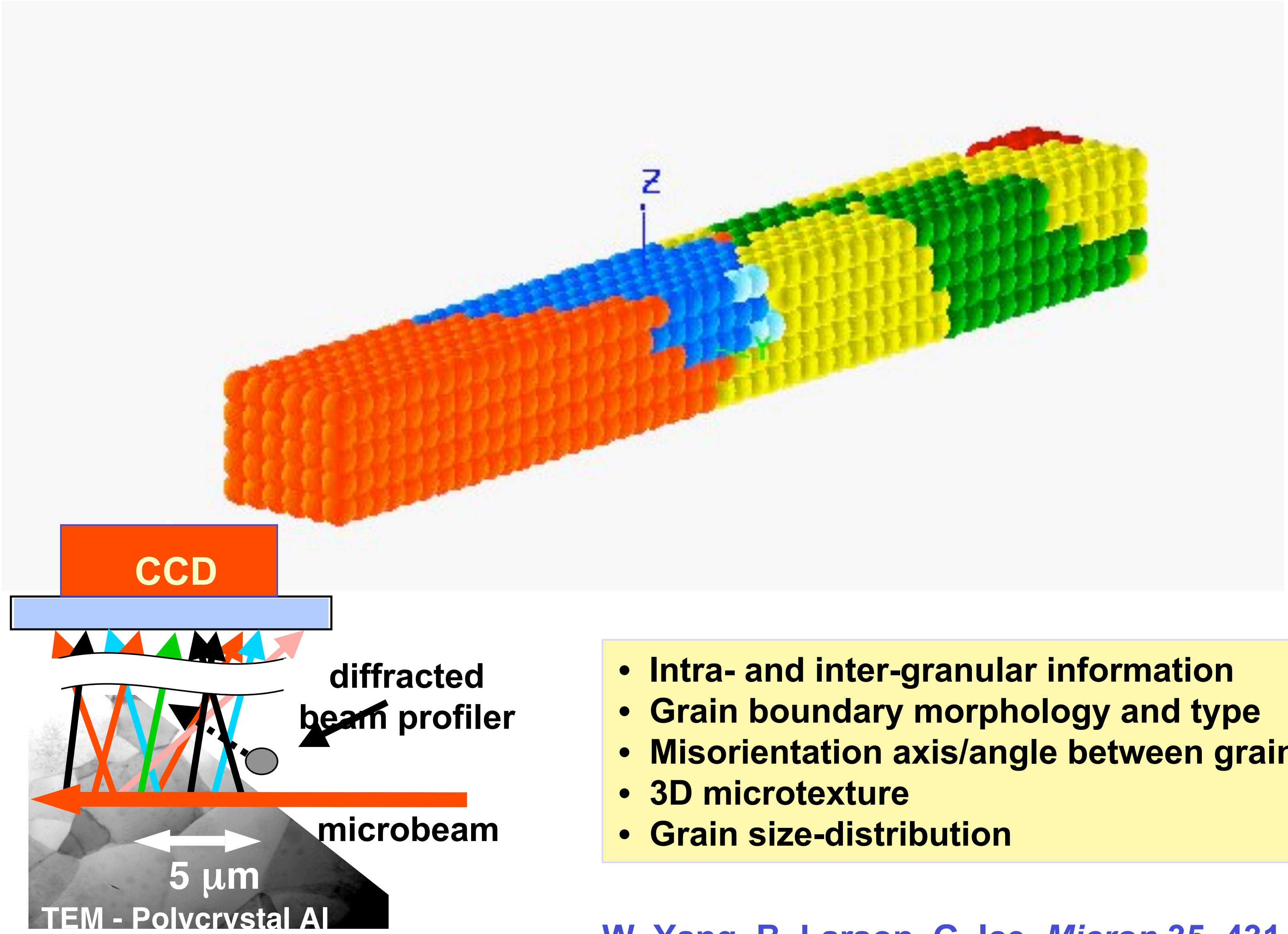

- Intra- and inter-granular information
- Grain boundary morphology and type
- Misorientation axis/angle between grains
- 3D microtexture
- Grain size-distribution

W. Yang, B. Larson, G. Ice, *Micron* 35, 431 (2004)

Real vs. reciprocal-space methods

- **Resolution of real-space methods is fundamentally limited by optics technology. Because n ~ 1 for x-rays, NA << 1 and DOF << R (like electrons).**

- **Reciprocal-space methods can benefit from high resolution detectors and optics ...**

  ⇒ But the resolution ultimately depends on neither.
  R and DOF are limited only by λ and usable signal.

Coherent diffraction microscopy

- X-ray coherent diffraction is a *lensless* method suited for 3D imaging of non-crystalline structures
- Resolution limited only by measurable momentum transfer (NA)
- But: have phase problem - full recovery is required, must assume some *a priori* information, e.g. object extent

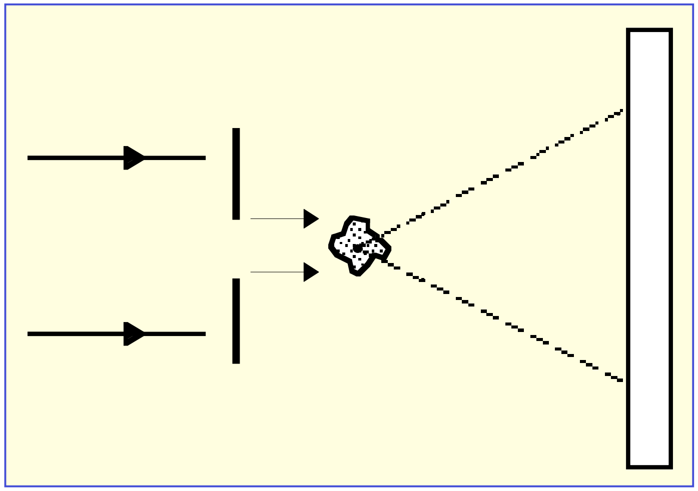

J. Miao et al., *Nature* 400, 342 (1999)

Diffraction approach

Record coherent diffraction pattern

$$I = |a|^2$$

- **Phase information is obtained by measuring diffraction pattern at sufficiently fine intervals**
- **Reconstruct object amplitude by guessing at phase, then iteratively improving guess to get self-consistent solution**
- **Resolution:** transverse $R \sim 0.61\ \lambda/NA$
  longitudinal $DOF \sim 1.22\ \lambda/(NA)^2$

Contrast: $\propto |f_1^2 + f_2^2|$

Phasing by iterative error reduction

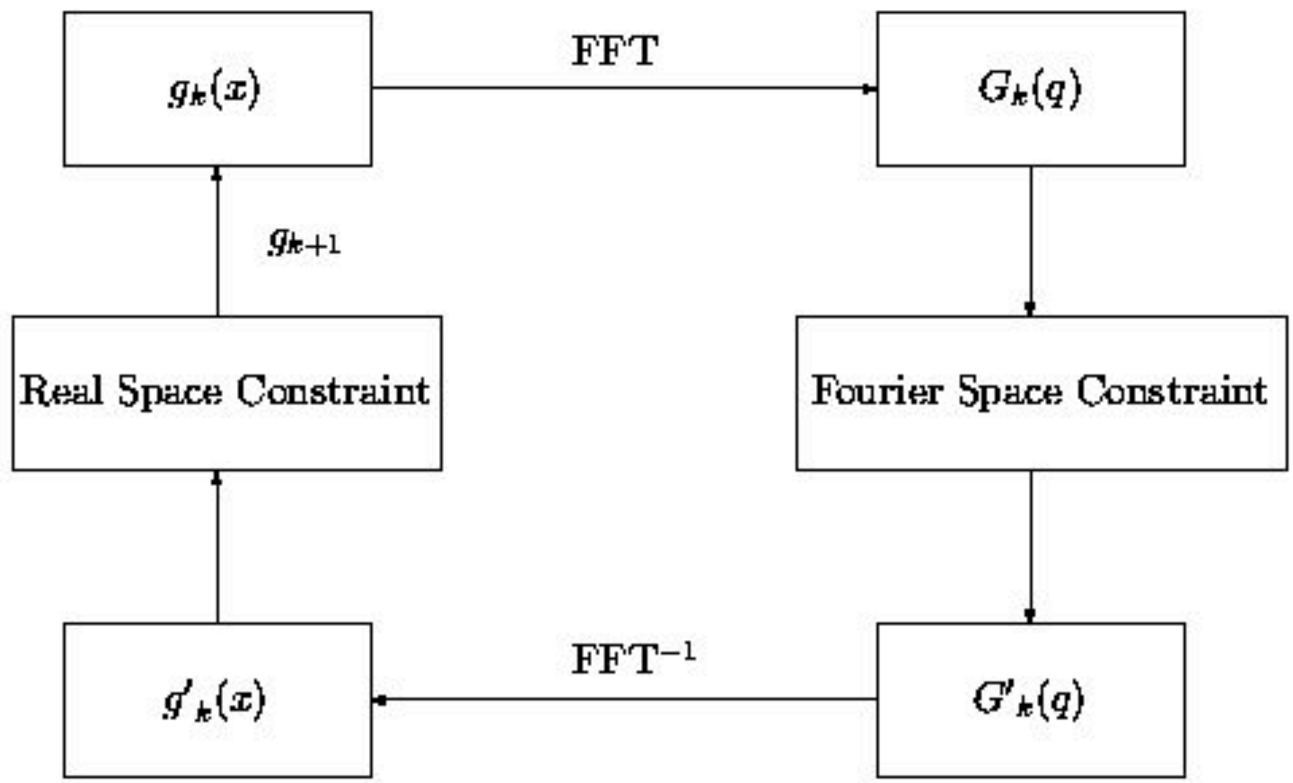

R. Gerchberg and W. Saxton, *Optik* 35, 237 (1972)
J. R. Fienup, *Appl. Opt.* 21, 2758 (1982)

Biological objects

Reconstructed coherent diffraction images of a freeze-dried yeast cell viewed at (A) normal, (C) 3°, and (D) 4° off-normal incidence. Labels identify the nucleus (N), a storage vacuole (V), and cell membrane (M). Image brightness represents magnitude, hue represents phase.

(B) STXM image taken of the same cell using 540-eV x-rays at ~42 nm resolution.

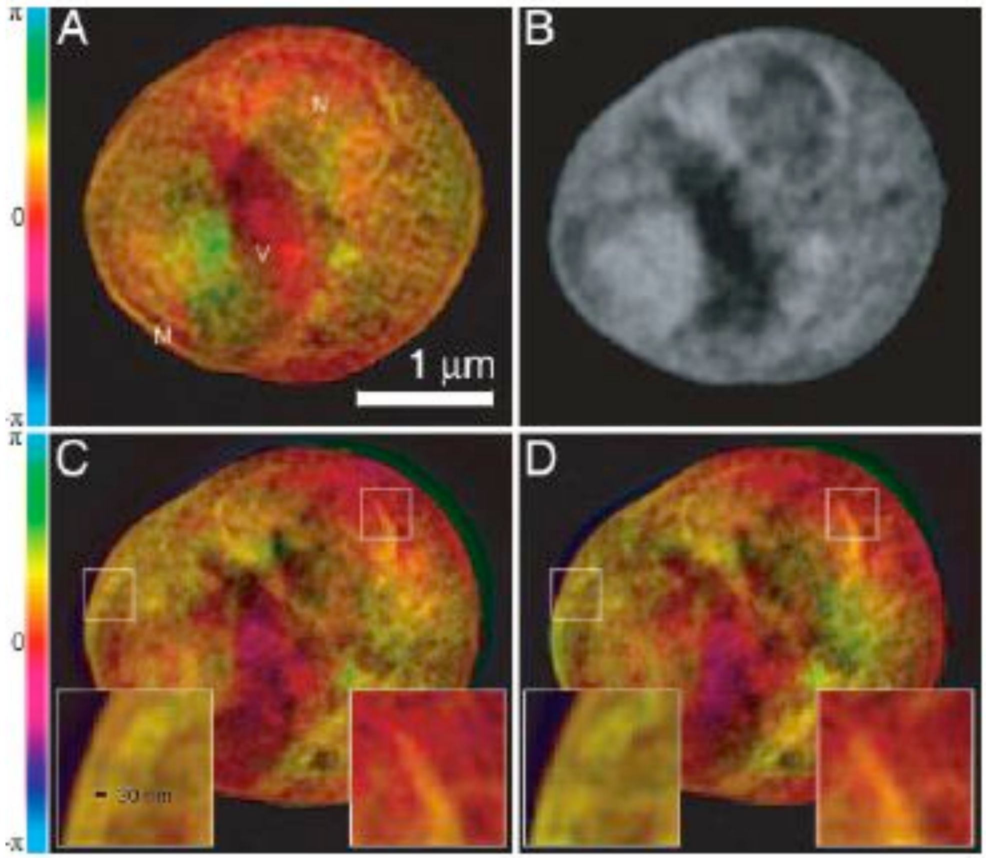

D. Shapiro et al., *PNAS* 102, 15343 (2005)

Optimizing sample contrast

- Optimizing contrast for biological specimens such as cytoskeletal actin filaments and mineralized fish bone
- Exploring resonant enhancement at absorption edges

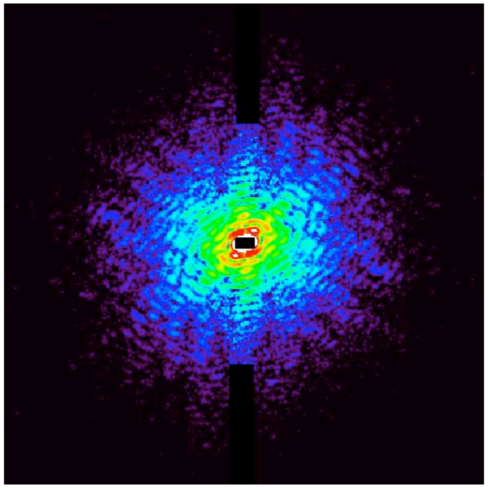

Coherent diffraction pattern (2.2 keV) from a fish bone at a low mineralization state

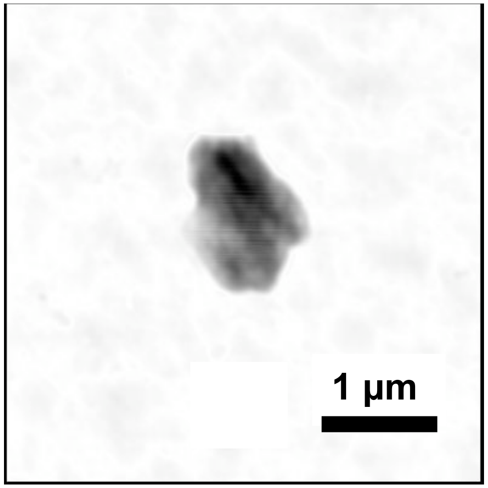

Image of fish bone reconstructed solely from diffraction data

J. Miao, C. Song (UCLA)

Holographic approach

Record hologram

$$I = |a+b|^2 = |a|^2 + |b|^2 + a^* b + a b^*$$

Reconstruct

$$\begin{aligned} bI &= b|a|^2 + b|b|^2 + a^* bb + abb^* \\ &= aI_b + b(I_a + I_b) + \text{background} \end{aligned}$$

- **Reference wave encodes magnitude and phase of wave scattered by object in hologram**
- **Contrast and resolution: same as for coherent diffraction**
- **Reconstruct sample amplitude by "re-illuminating" hologram with reference wave (or its C.C.)**

Holography

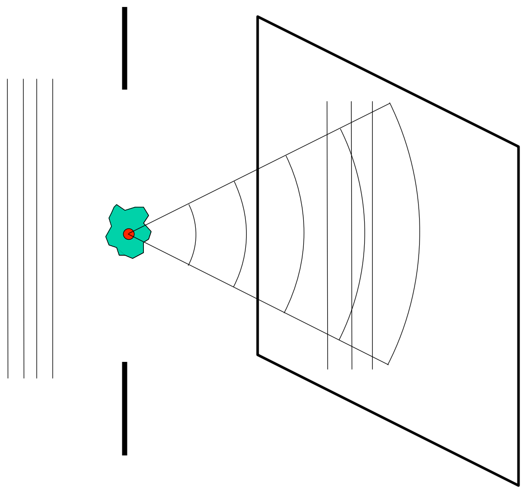

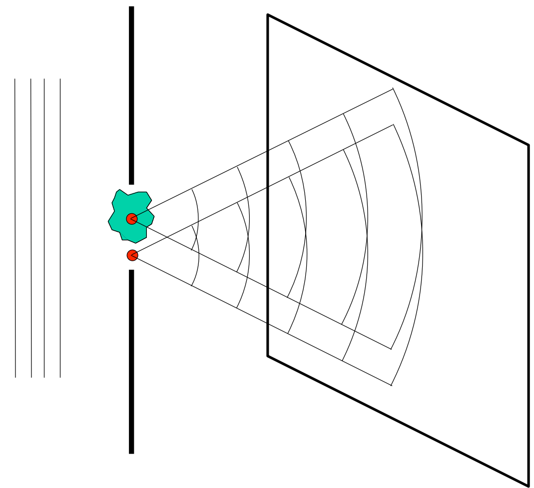

Gabor

plane reference wave
(in-line)

Fourier Transform

spherical reference wave
(off-axis)

D. Gabor, *Nature* 161, 777 (1948)

G. Stroke, *Appl. Phys. Lett.* 6, 201 (1965)
Winthrop, Worthington, *Phys. Lett.* 15, 124 (1965)

FT hologram formation

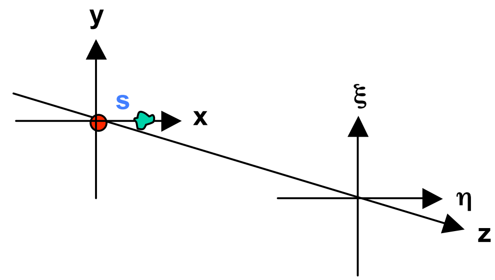

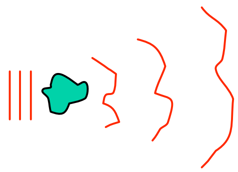

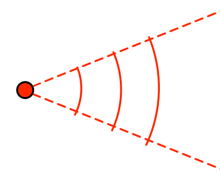

$$a(\xi,\eta) = \frac{e^{ikz}}{i\lambda z}\iint a(x-s,y)e^{-\frac{ik}{2z}\left((x-\xi)^2+(y-\eta)^2\right)}dxdy$$

object wave

$$b(\xi,\eta) = \frac{e^{ikz}}{i\lambda z}b_0 e^{\frac{ik}{2z}\left(\xi^2+\eta^2\right)}$$

reference wave

$$I = |a+b|^2 = |a|^2 + |b|^2 + a^* b + ab^*$$

hologram intensity

Reconstruction

- **Numerically take FT of hologram intensity to reconstruct**
- **Spatially separated primary, conjugate object waves result**
- **Weak curvature f(x,y) on object wave can be ignored**

Image terms: $$a^*b+ab^* = \varphi(s\xi)F(\xi,\eta)+\varphi(s\xi)^*F(\xi,\eta)^*$$

where: $$F(\xi,\eta) = \frac{e^{ikz}}{i\lambda z} f(\xi,\eta)\iint a(x,y)f(x,y)e^{-\frac{ik}{z}(x\xi+y\eta)}dxdy \quad ,$$

$$\varphi(s,\xi) = e^{-\frac{ik}{z}s\xi} \quad \textbf{and} \quad f(\xi,\eta) = e^{\frac{ik}{2z}\left(\xi^2+\eta^2\right)}$$

$$FT^{-1}\left\{a^*b+ab^*\right\} = \boxed{f(x-s,y)\,a(x-s,y)} + f(-(x-s),-y)^*\,a(-(x-s),-y)^*$$

Hard disks: storage density

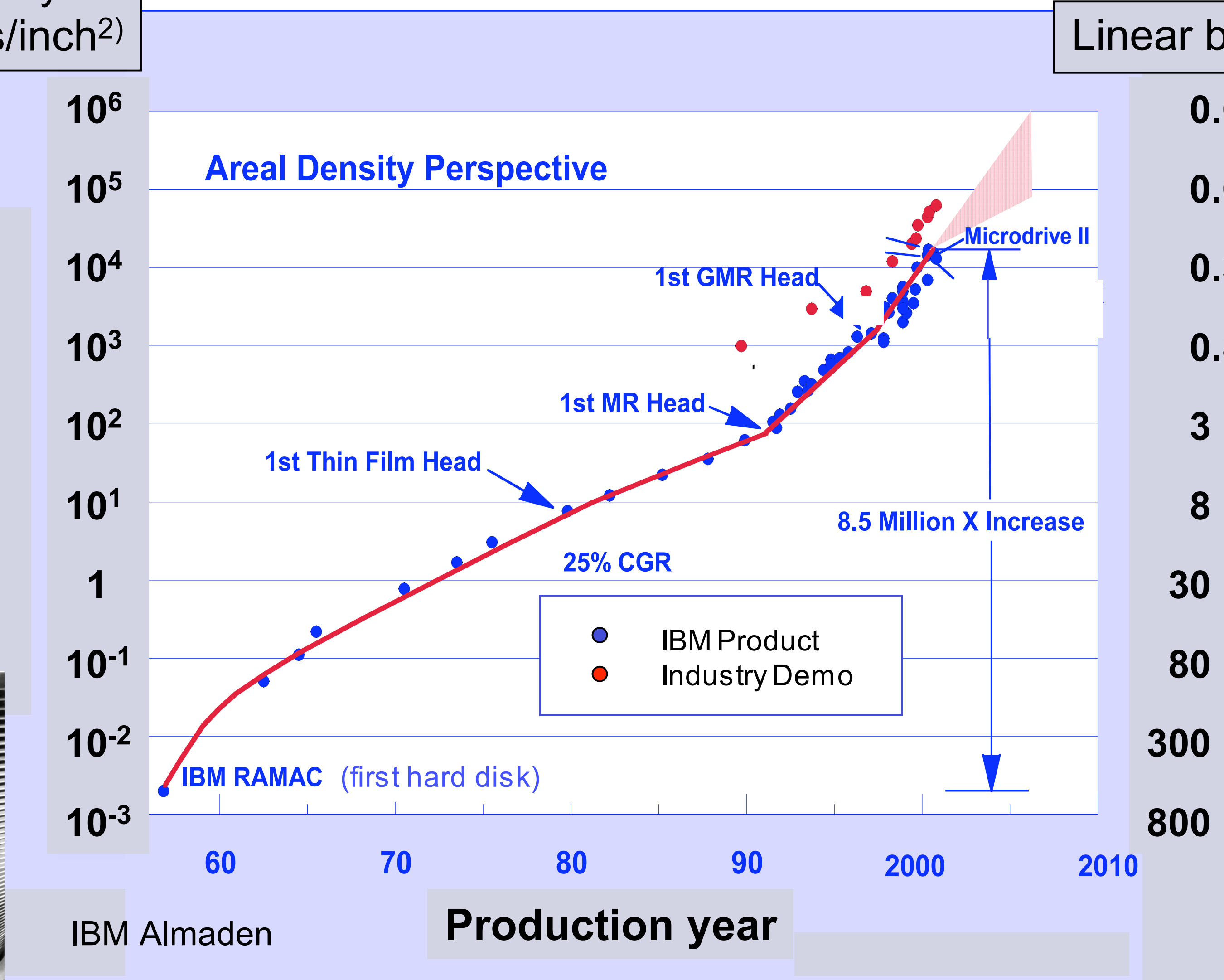

CoPt magnetic labyrinth nanostructures

side view

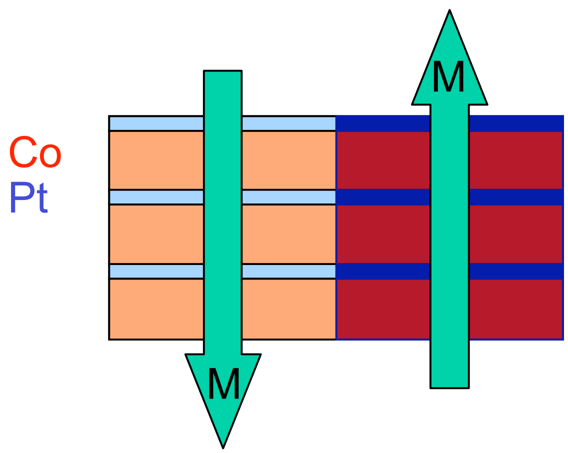

Sample: O. Hellwig (Hitachi)

MFM, top view

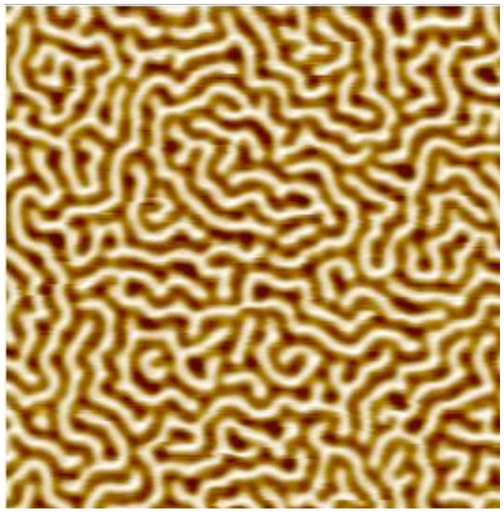

5 μm x 5 μm

continuous object

SiN_x / Pt (24 nm) /
[Co (1.2 nm) / Pt (0.7 nm)]$_{50}$ /
Pt (1.5 nm)

perpendicular anisotropy → magnetic storage media

Pinhole mask method

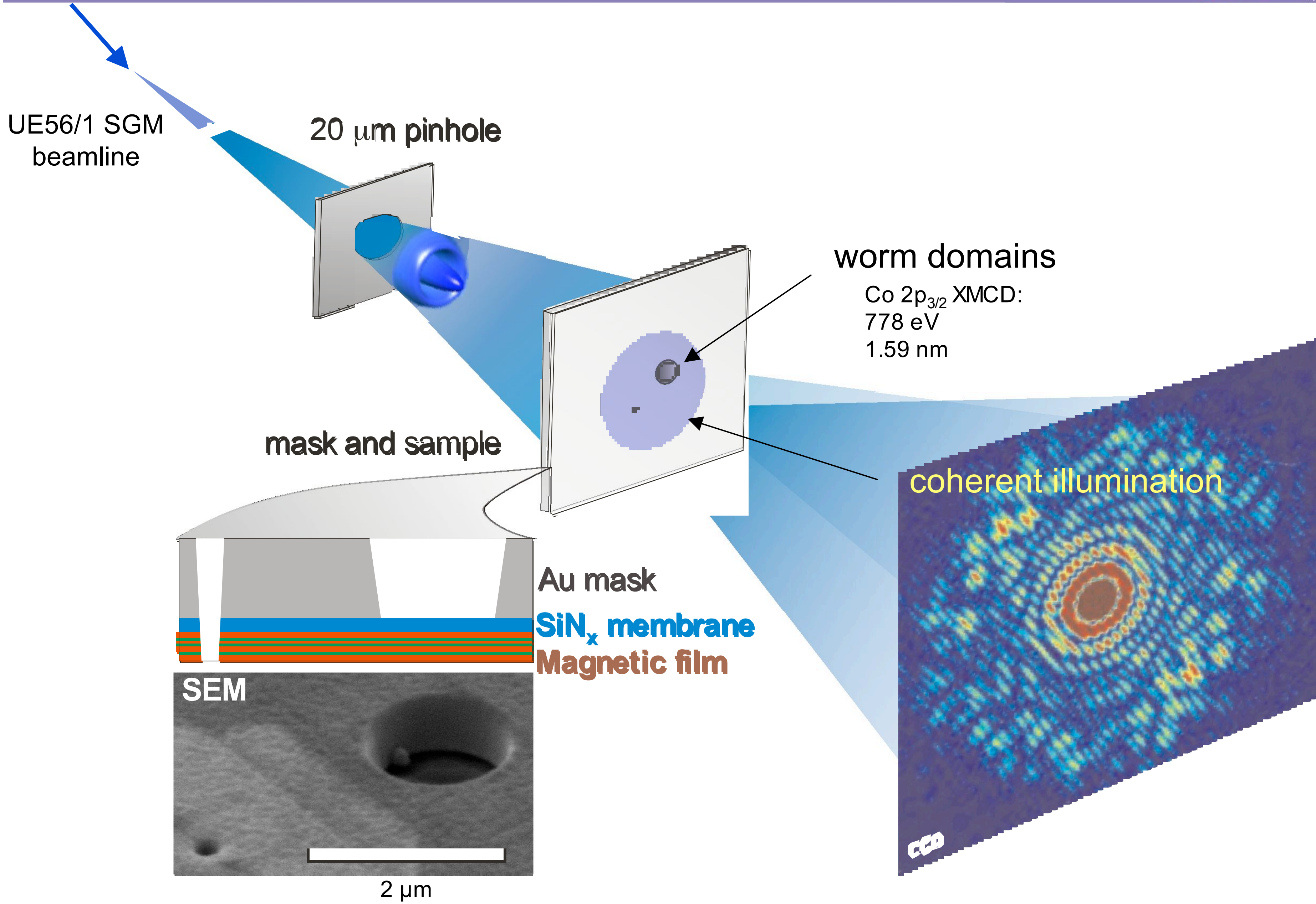

FTH

STXM

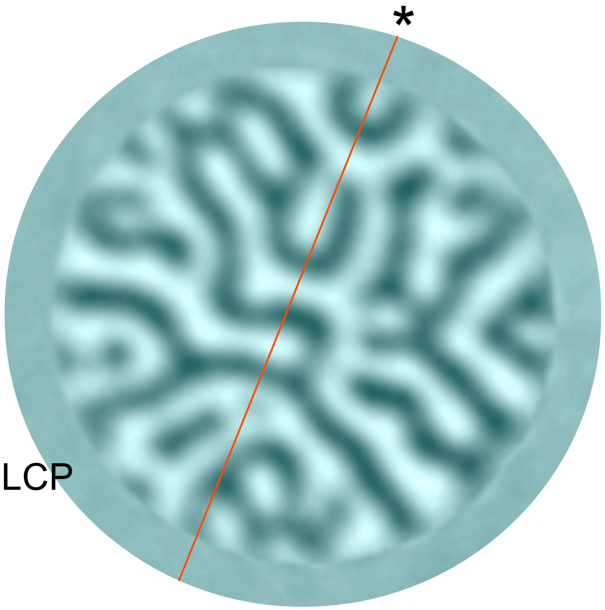

$\varnothing$ 1.5 μm

100 nm

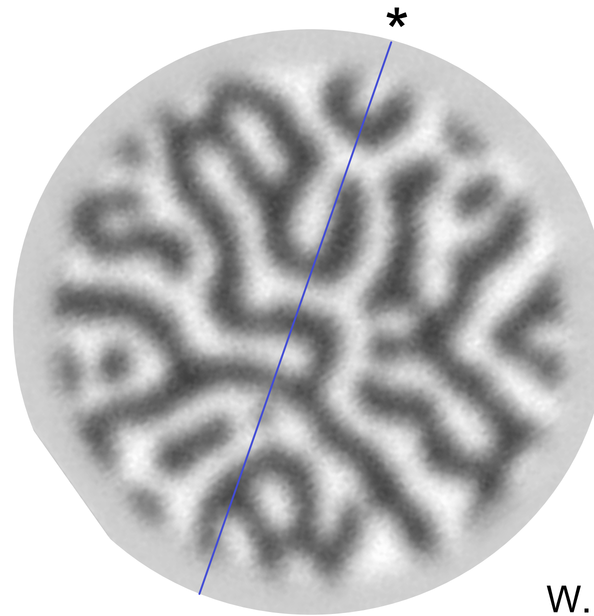

W. Schlotter
Y. Acremann

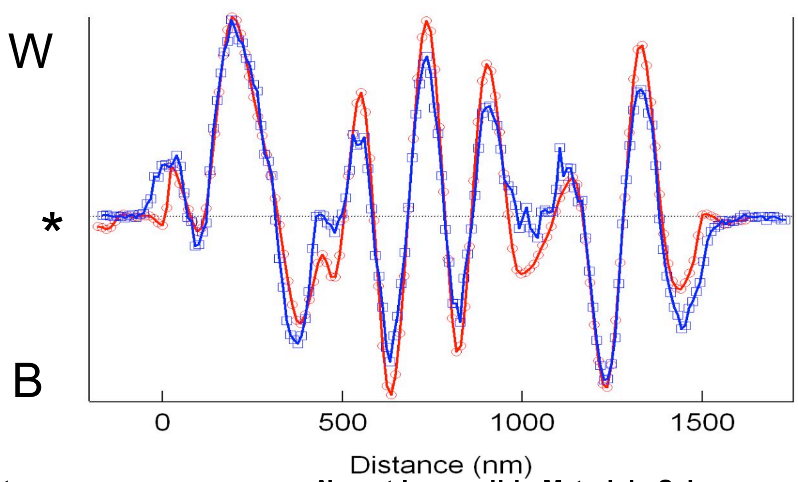

Reconstructed resolution ~50 nm

Resolution 30-40 nm

S. Eisebitt et al., *Nature* 432, 885 (2004)

Switching in patterned magnetic media

LETTERS

Magnetic multilayers on nanospheres

MANFRED ALBRECHT[1]*, GUOHAN HU[2], ILDICO L. GUHR[1], TILL C. ULBRICH[1], JOHANNES BONEBERG[1], PAUL LEIDERER[1] AND GÜNTER SCHATZ[1]

Nature Materials 4, 203 (2005)

a

Deposition direction

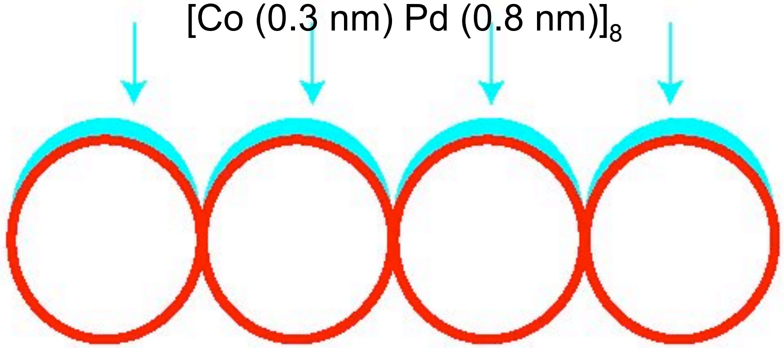

$\varnothing$ 330 nm

b

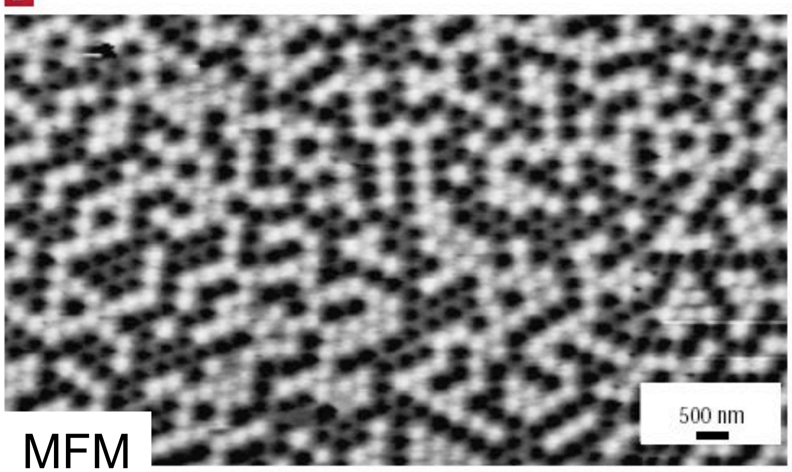

MFM

$\varnothing$ 110 nm

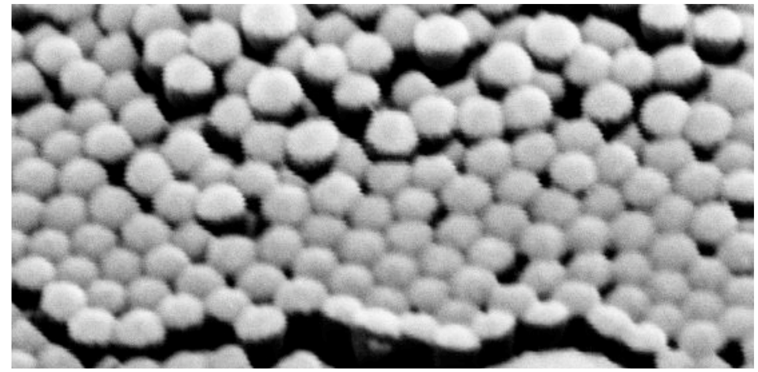

SEM

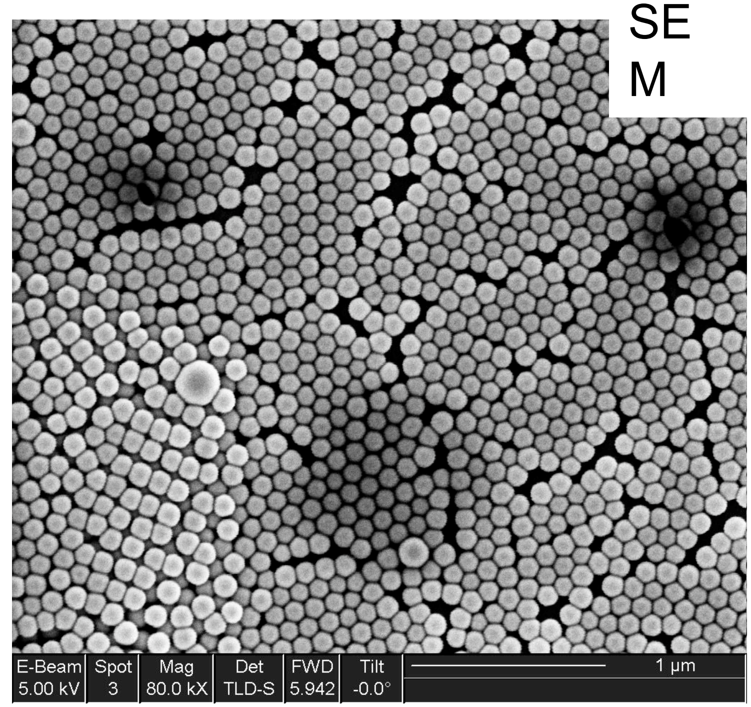

Nanostructure of multi-twinned crystals

- Multi-twinned Pb crystals >5 μm in size are readily grown by electrodeposition. Morphology is strongly dependent on the electrochemical potential

- Calculations indicate they should not grow larger than ~200 nm due to strain near grain boundaries

- Even highly regular “crystals” show little or no Bragg diffraction

- If crystals, what is their structure, orientation, and nature of defects?

- Are they amorphous?
  If so, how do they grow?

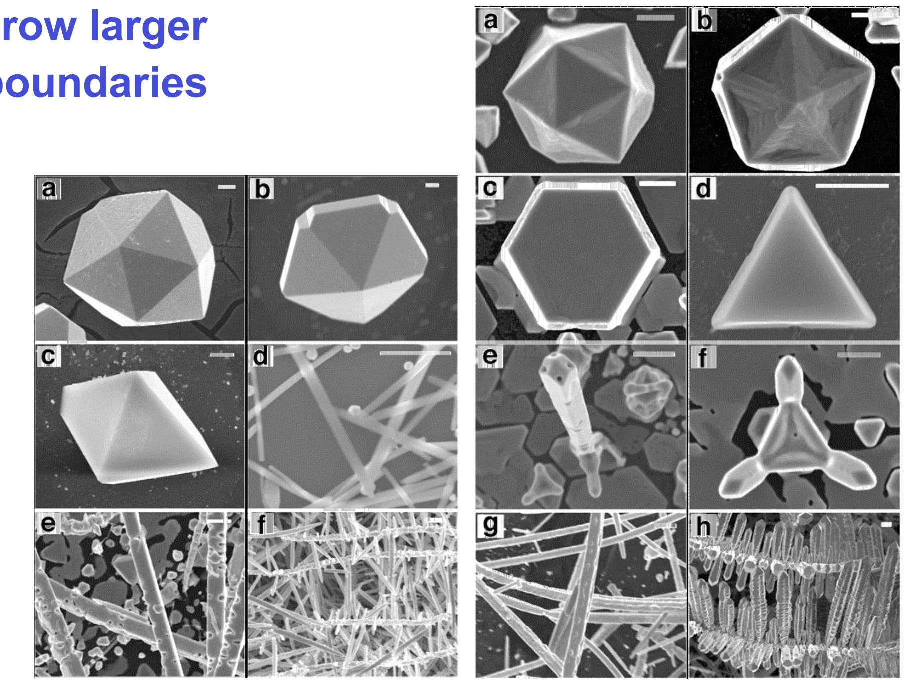

Z. Xiao et al., *J. Am. Chem. Soc.* 126, 2316 (2004)

Fourier transform experiment

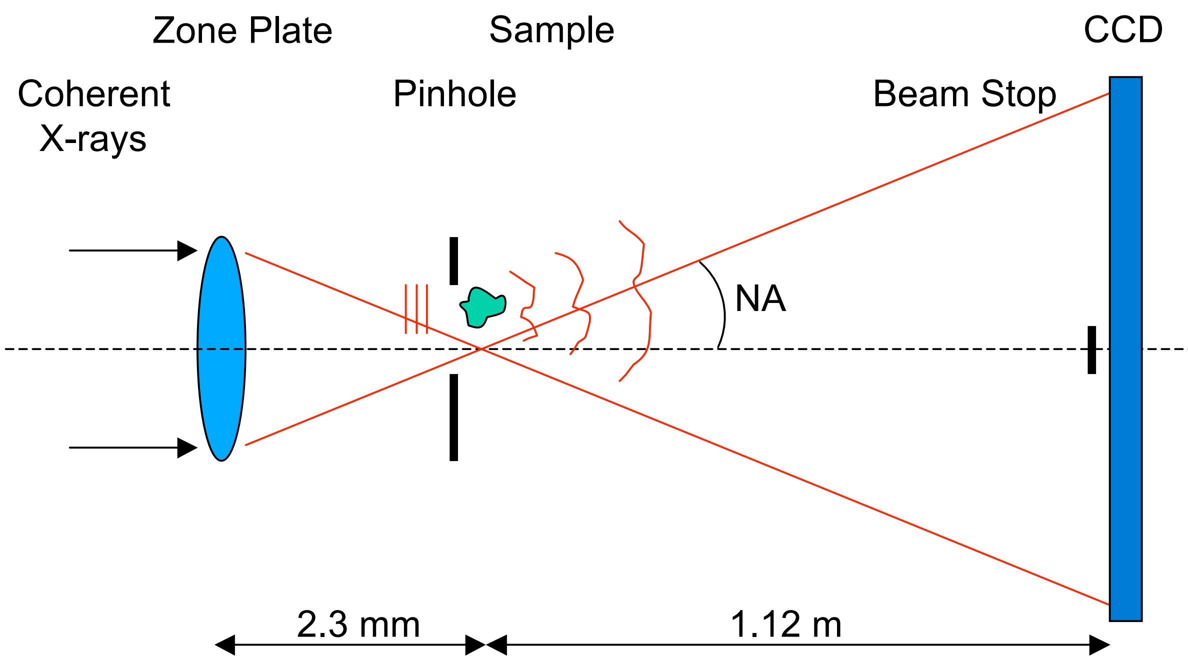

- Beam passing through zone plate (0th-order) illuminates sample.
- Beam focused by zone plate (3rd-order) serves as reference. Reference wave interferes with object wave to form hologram.
- NA of reference wave determines hologram resolution. Detector resolution determines object field of view.

Sample

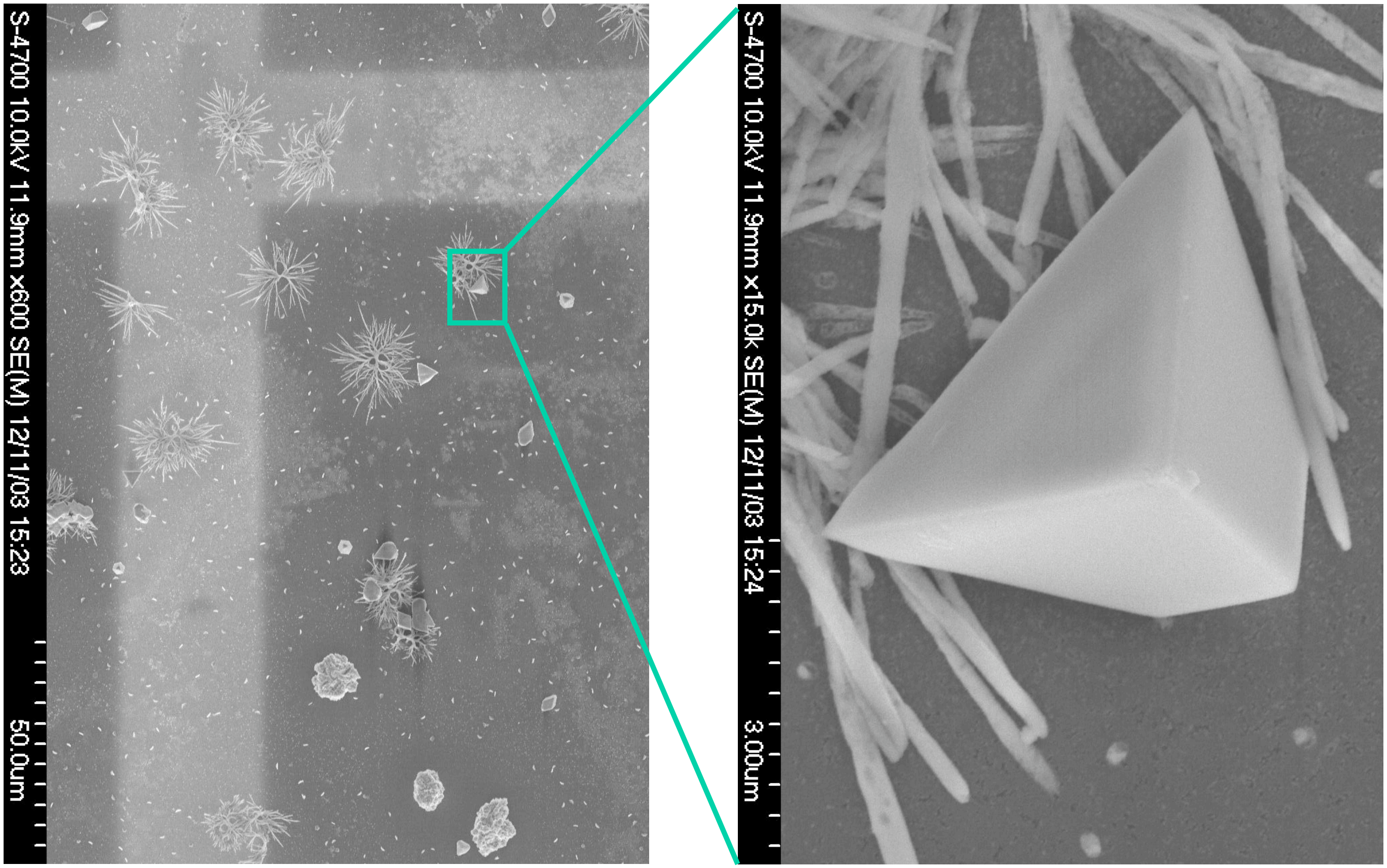

Y. Xiao (APS), Z. Xiao (ANL/MSD)

Holograms

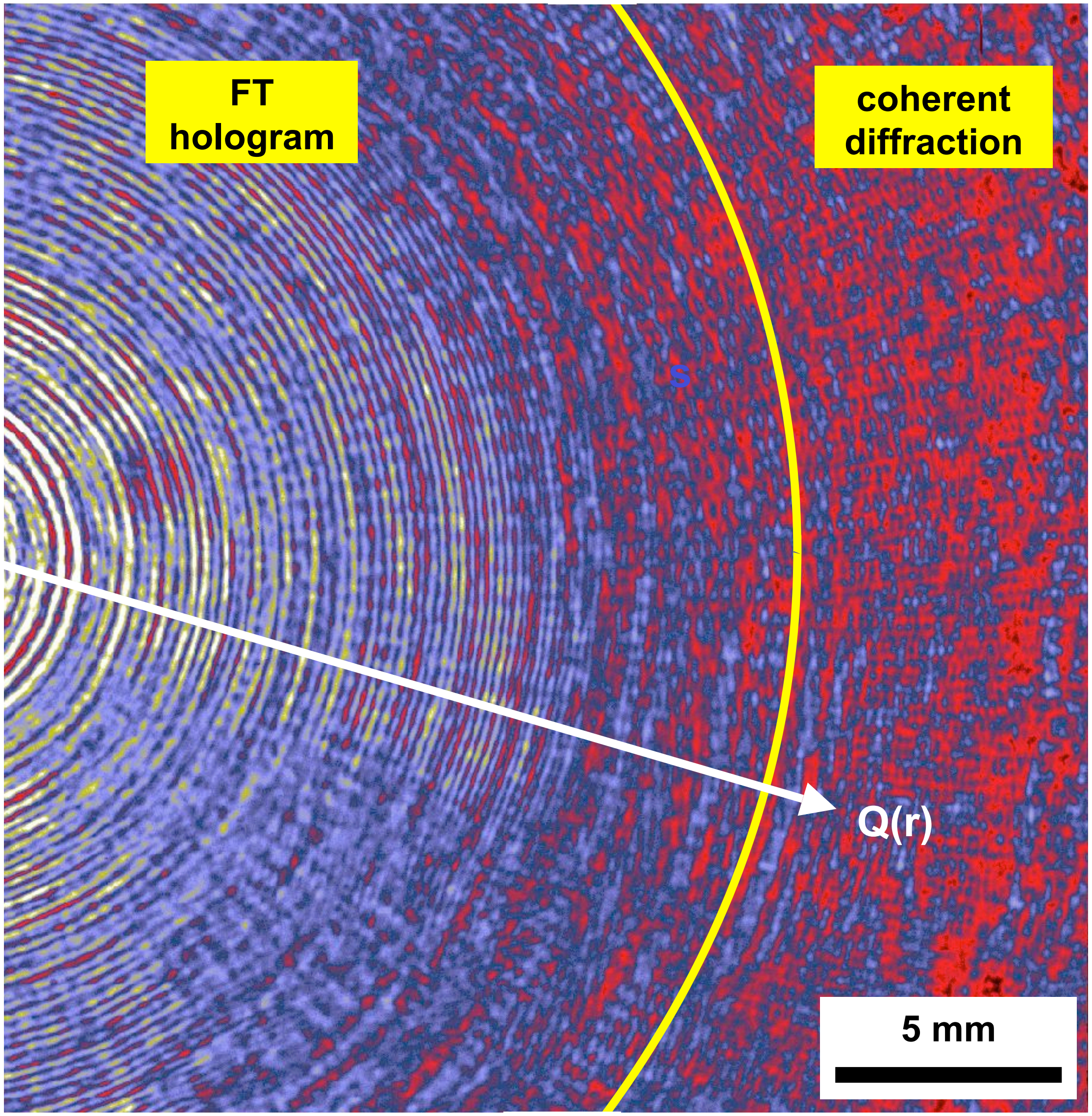

Only *part* of hologram recorded

- **limit direct-beam blooming**
- **increase angular resolution**
- **collect un-phased diffraction**

... but pay penalty:

- **much sample information not recorded, especially at lowest spatial resolution**

Reconstructed holograms

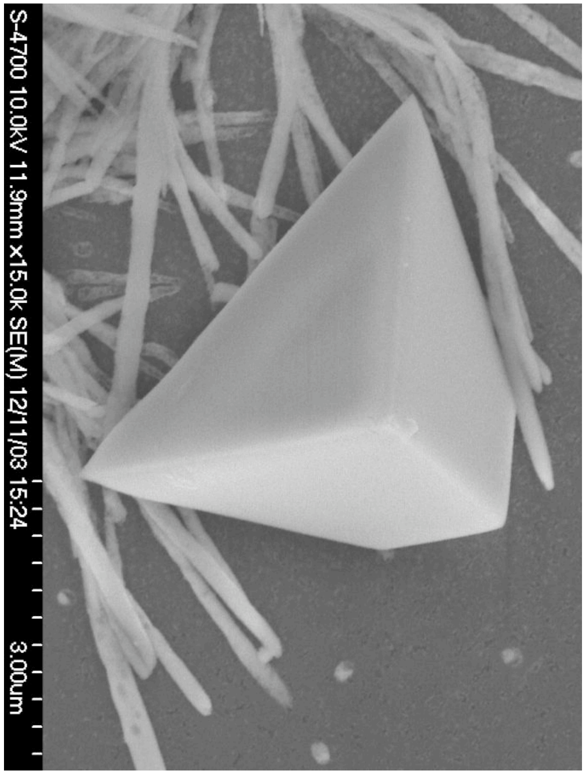

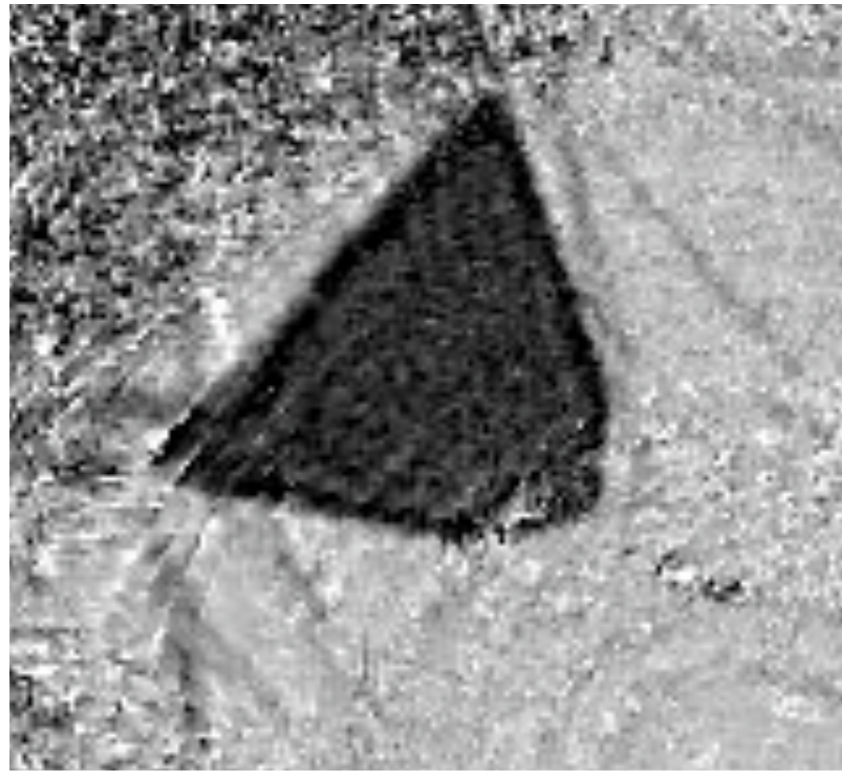

3 µm

Closeup SEM of Pb crystal. Crystal is ~4.5 µm in extent; dendrites are 100-300 nm wide.

Reconstructed FT hologram. Field of view is limited to ~5 µm by detector resolution. X-ray energy was 1050 eV.

Finer structures are resolved with phase

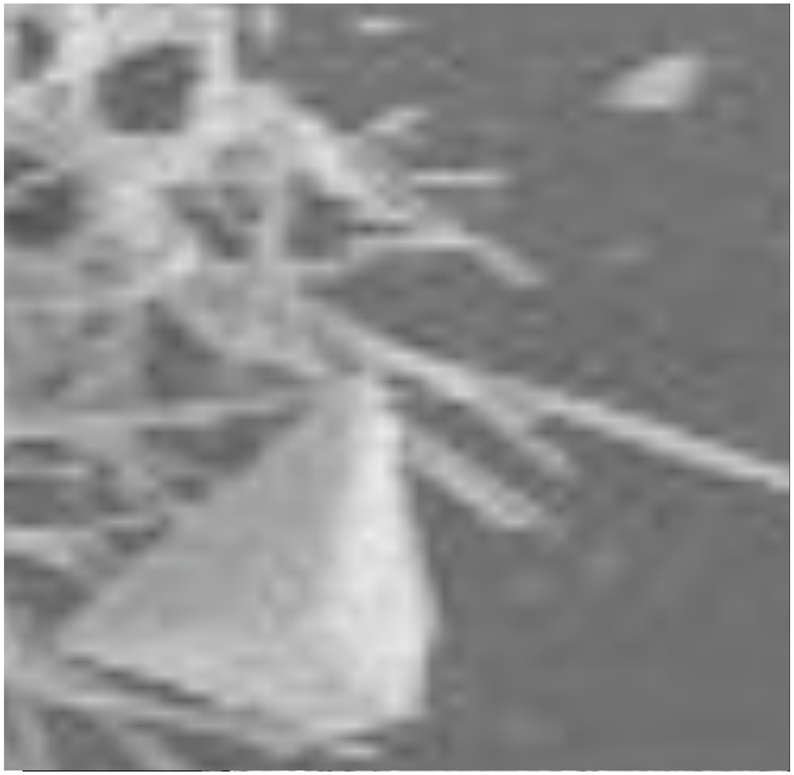

Magnitude

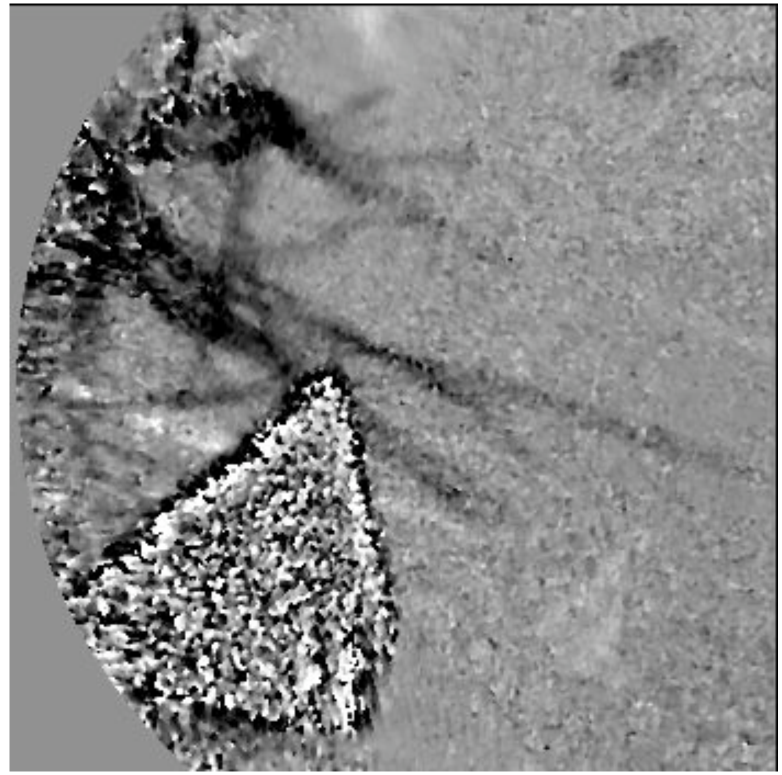

Phase

$$\text{phase} = \tan^{-1}\left\{\frac{\text{Im}\,(\psi)}{\text{Re}\,(\psi)}\right\}$$

Coherent diffraction is aided by Fresnel

G. Williams, K. Nugent (U. Melbourne)

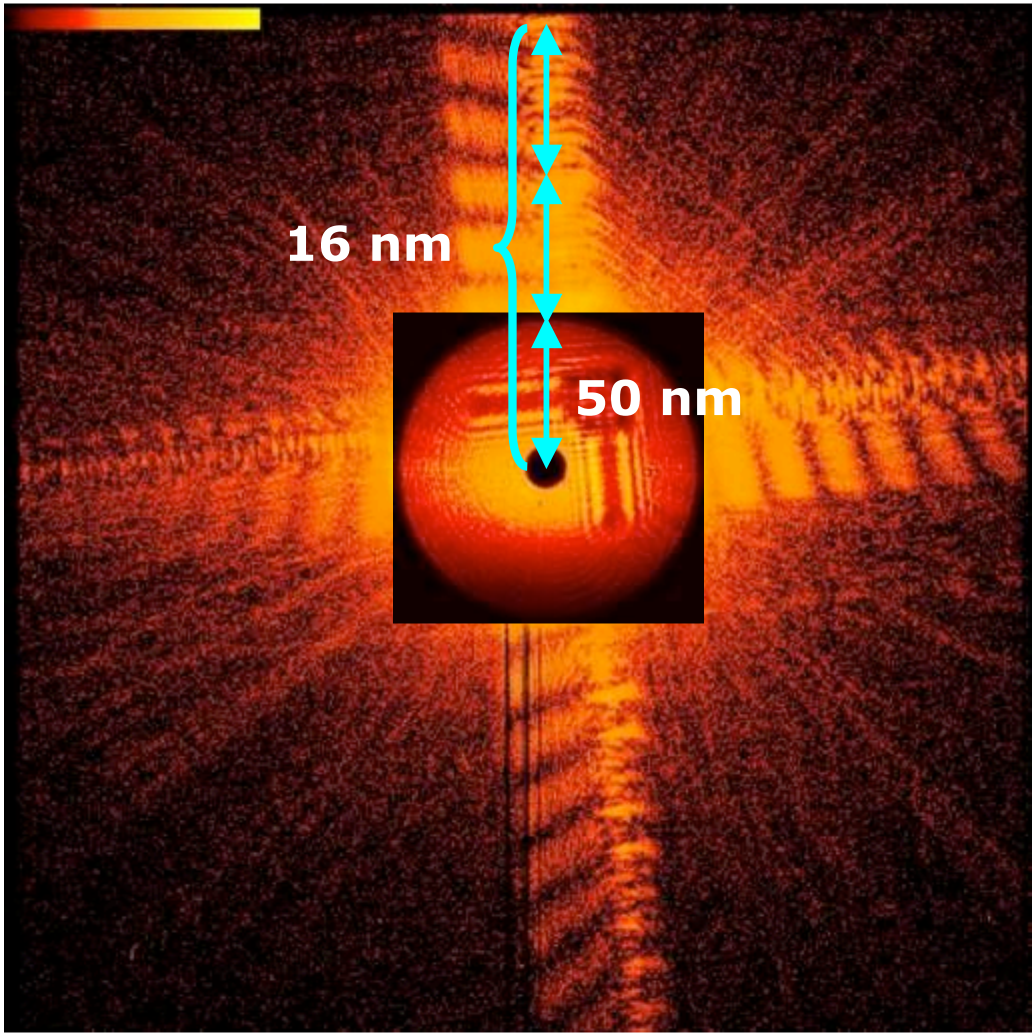

Fresnel diffraction imaging

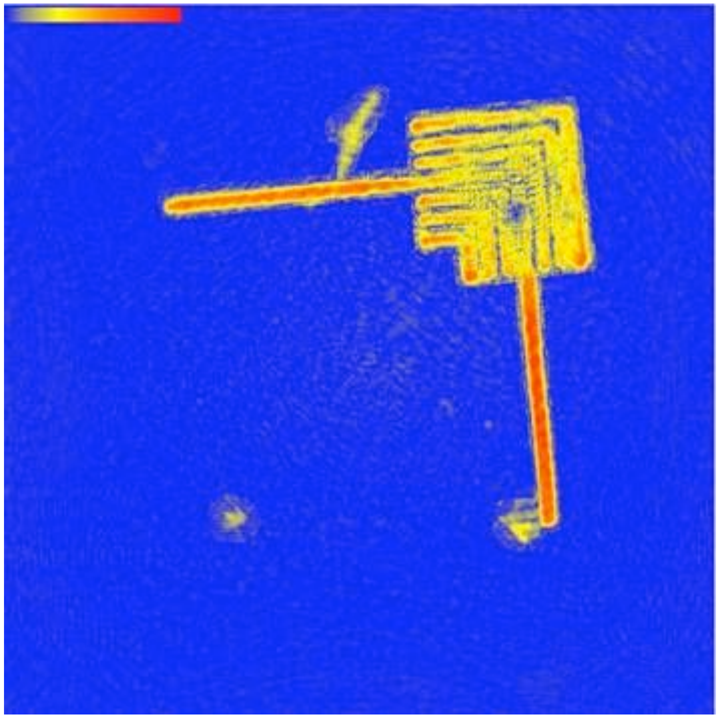

Phase

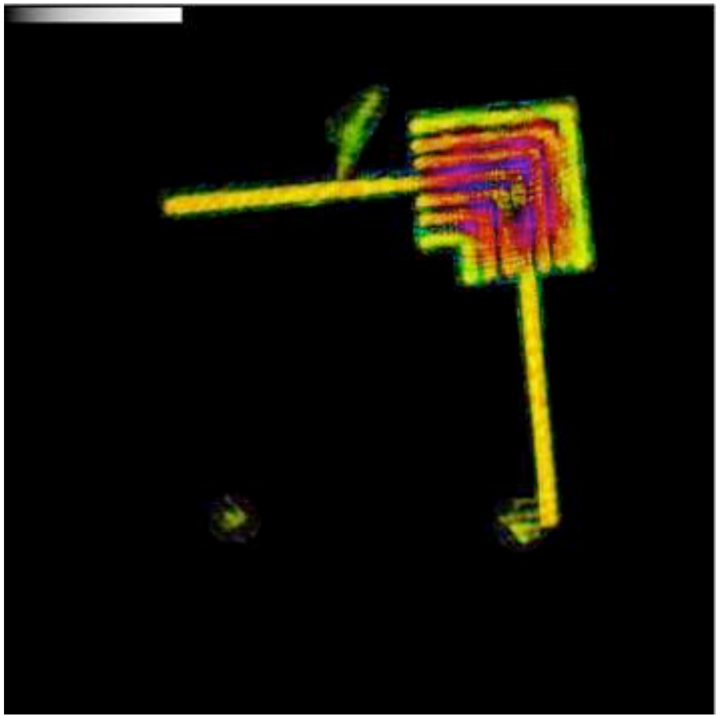

Magnitude with color-encoded phase

3D coherent diffraction microscopy

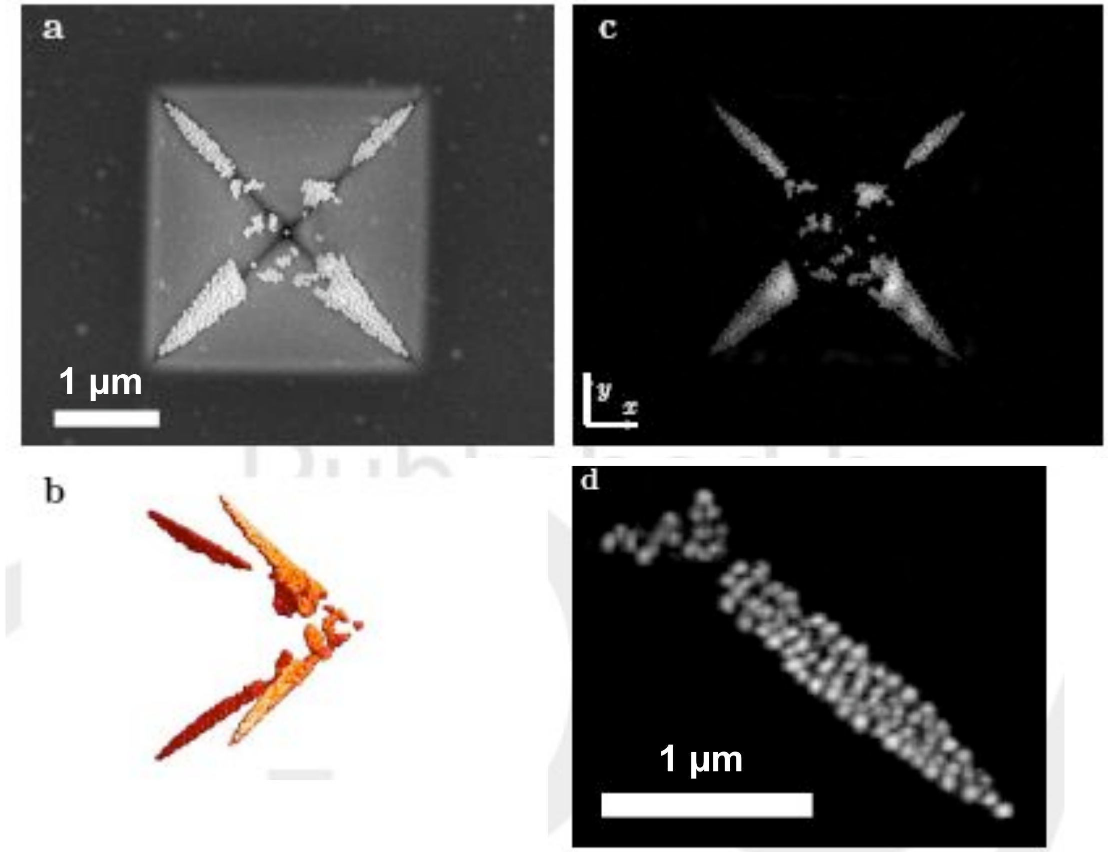

(a) SEM of pyramidal indentation in a 100-nm Si_3N_4 membrane lined with 50-nm Au spheres. (b) 3D image reconstructed from 123 diffraction projections spanning -57° to +66°, using reality and positivity constraints. (c) Large DOF projection. (d) Enlarged region of (c).

H. Chapman et al., *J. Opt. Soc. Am.* A23, 1179 (2006)

3D coherent diffraction microscopy

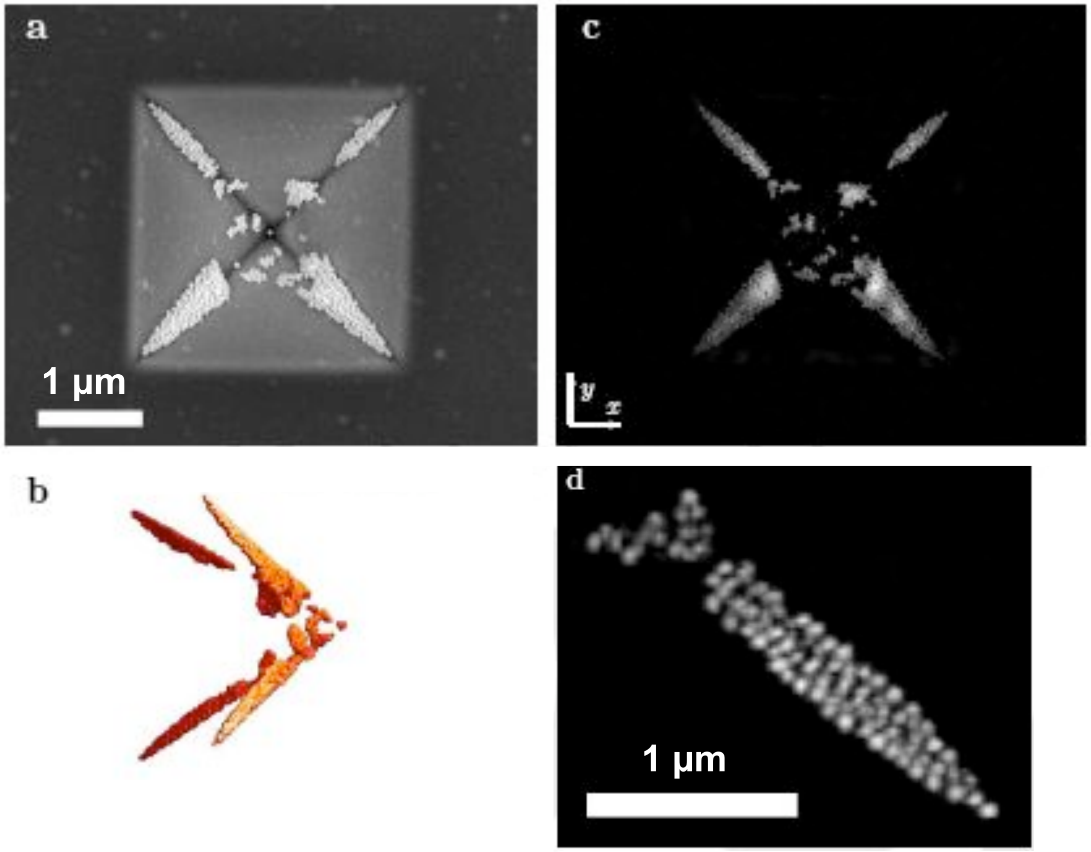

(a) SEM of pyramidal indentation in a 100-nm Si_3N_4 membrane lined with 50-nm Au spheres. (b) 3D image reconstructed from 123 diffraction projections spanning -57° to +66°, using reality and positivity constraints. (c) Large DOF projection. (d) Enlarged region of (c).

H. Chapman et al., *J. Opt. Soc. Am.* A23, 1179 (2006)

Tomography at the nanoscale

Technically challenging

- Precision sample rotation and targeting in x,y,z
- Short working distance at high NA (using optics)
- Radiation dose to sample (but Dose fractionation helps)

Physical limitations restrict

- Accessible angular range
- Number of views obtainable
- Sample field-of-view

... time consuming!

⇒ Parallelize projection acquisition

Multi-view holography with beamsplitter

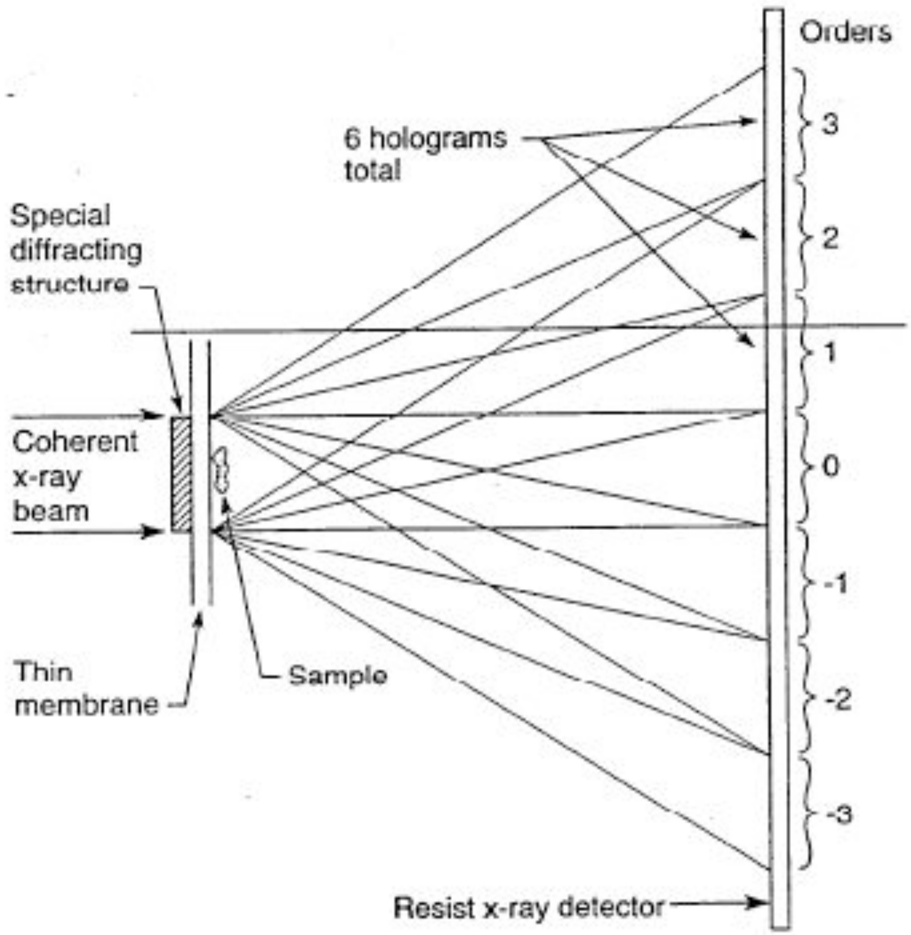

M.R. Howells,
Proc. LCLS Workshop (1994)

Livermore team developed multiview method using several (e.g. 4) off-axis ZPs

Possible method for one-shot tomography. Six holograms are shown but they are part of a 2D array of 7x7-1 = 48

Multiple illumination directions

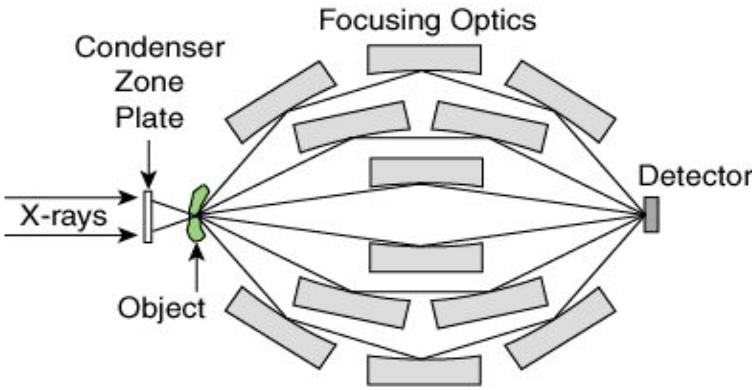

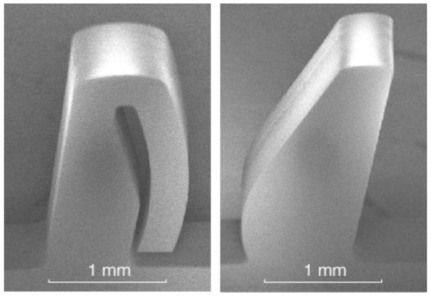

Micromachined Si mirror nano-actuators for x-ray astronomy

M. Schattenberg, MIT

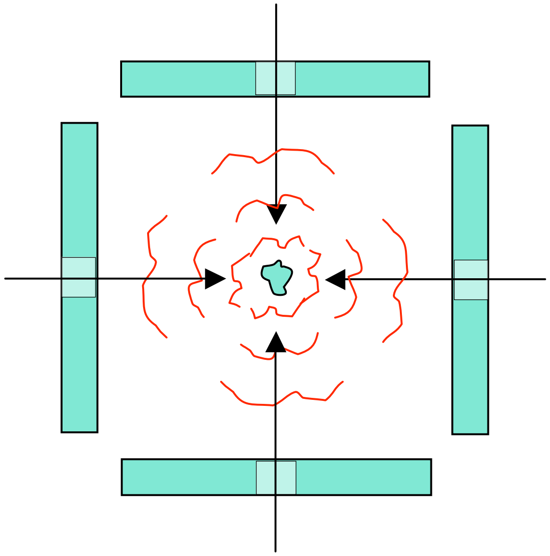

Parallel tomographic coherent diffraction. N beams are directed through sample onto N detectors

What we've learned

- **Coherent diffraction microscopy is getting easier, but phase retrieval is slow and uniqueness problem not solved.**
- **Holograms are quickly and reliably reconstructed in seconds on a small computer. Pinholes give cleanest results, but ZPs are best for sample and scalable to hard x-rays. Holographic data aids diffraction phase recovery.**
- **Currently takes ~10^{10} photons for ~50 nm resolution (2D). ERL should provide enough coherent flux for 3D data set at same resolution and in same time.**

Snapshots: smaller & faster

Stanford 1878

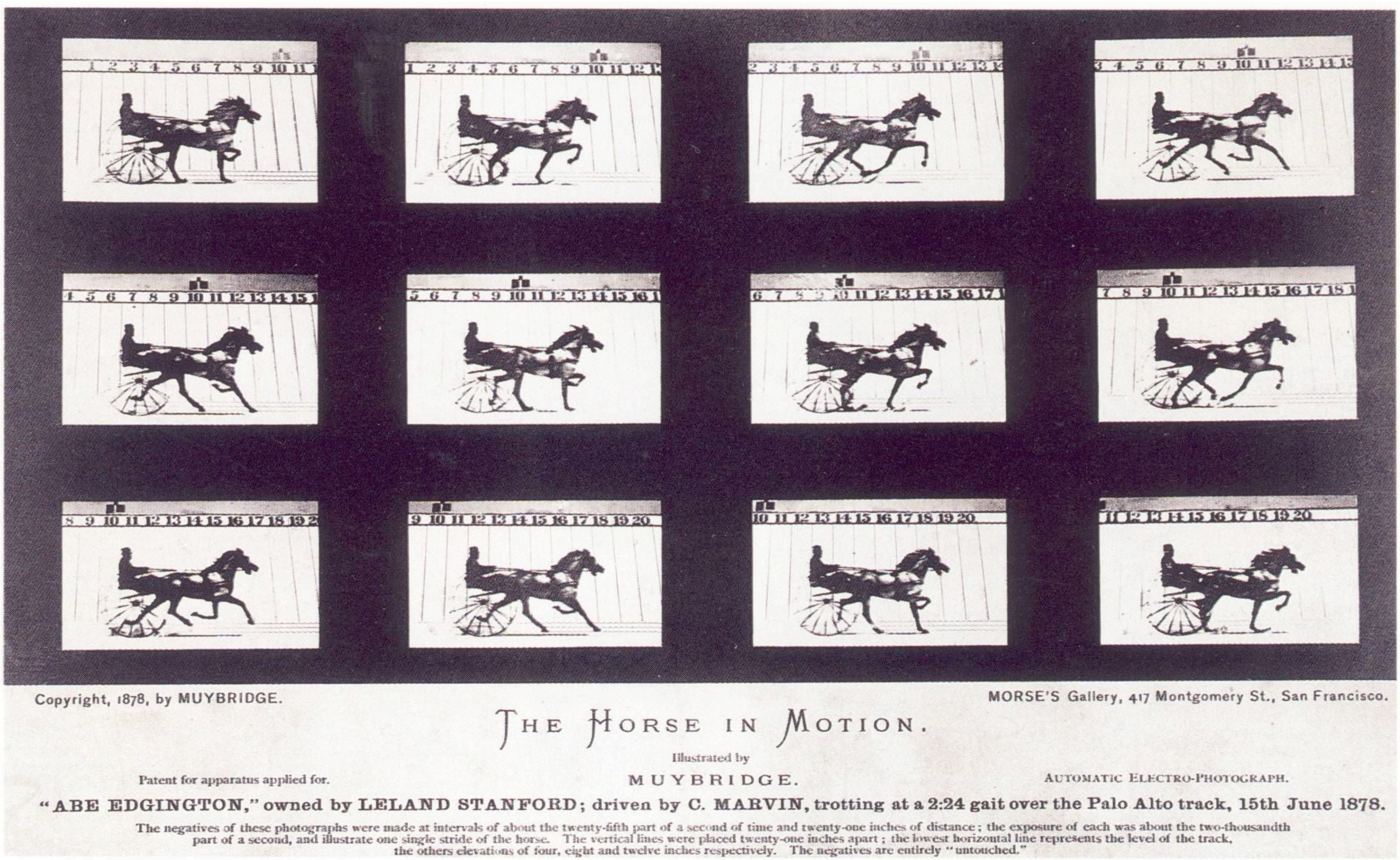

One day ... ps magnetic imaging?

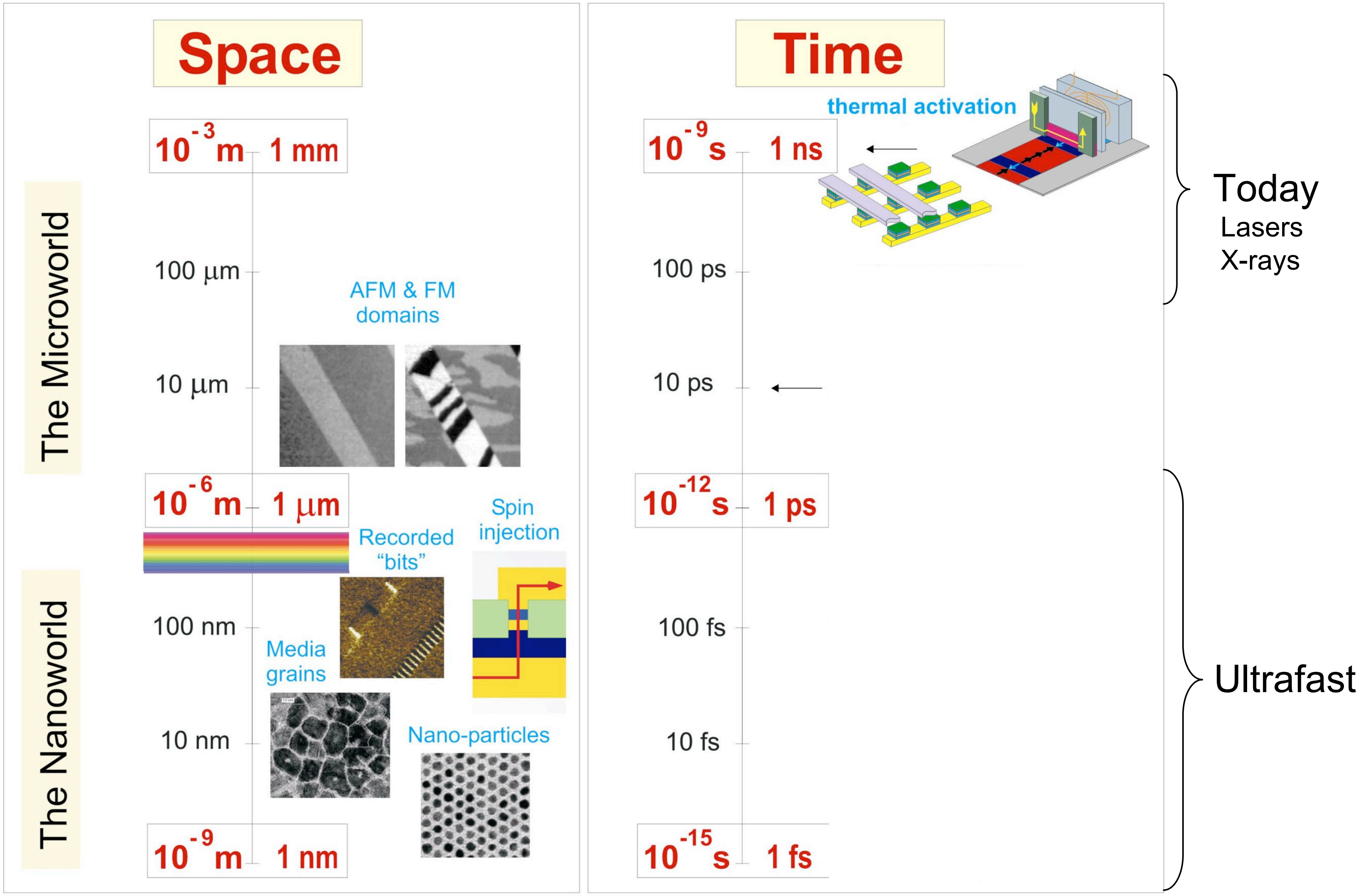

J. Stohr (Stanford U.)

Conclusions

- **X-ray microscopy is now being used to image nanoscale 3D structures at 3rd-generation sources, but acquisition takes days.**
- **Coherent diffraction avoids optics limitations and can be combined with tomography for 3D imaging. Parallel data collection will enable time-resolved studies.**
- **Materials science at the nanometer scale, especially time-resolved problems, will benefit from the 1000x higher brilliance of the ERL.**

Acknowledgements

Stefan Eisebitt, Chris Günther, Andreas Menzel, Florin Radu	BESSY
Lixin Fan, Yanan Xiao	Advanced Photon Source
David Paterson	Australian Synchrotron
Jianwei Miao, Changyong Song	U. California at Las Angeles
Keith Nugent, Andrew Peele	University of Melbourne
Bill Schlotter	Stanford University
Olaf Hellwig	Hitachi Almaden Res. Center

BESSY, EU Marie Curie Foundation, U.S. Dept. of Energy OS-BES